

# NATIONAL ADVISORY COMMITTEE FOR AERONAUTICS

TECHNICAL MEMORANDUM 1404

## INVESTIGATION OF APERIODIC TIME PROCESSES WITH AUTOCORRELATION AND FOURIER ANALYSIS

By Marie Luise Exner

Translation

"Untersuchung unperiodischer Zeitvorgänge mit der Autokorrelations-  
und der Fourieranalyse." Acustica, Bd. 4, Nr. 3, 1954.



Washington

March 1958

AFMDC  
TECHNICAL LIBRARY  
AFL 2811



## NATIONAL ADVISORY COMMITTEE FOR AERONAUTICS

## TECHNICAL MEMORANDUM 1404

## INVESTIGATION OF APERIODIC TIME PROCESSES WITH AUTOCORRELATION

## AND FOURIER ANALYSIS \*

By Marie Luise Exner

## SUMMARY

Autocorrelation and frequency analyses of a series of aperiodic time events, in particular, filtered noises and sibilant sounds, were made. The position and band width of the frequency ranges are best obtained from the frequency analysis, but the energies contained in the several bands are most easily obtained from the autocorrelation function.

The mean number of zero crossings of the time function was determined from the curvature of the latter function in the vicinity of the zero crossing, and also with the aid of a decimal counter. The second method was found to be more exact.

1. INTRODUCTION

For the analysis of voice sounds, practically the only method applied up to this time has been the Fourier analysis of the time process according to frequency. For vowels and other noises with predominantly periodic components, the analysis of the sound is undoubtedly the most suitable for the problem. The voiceless consonants are, however, only slightly periodic, and it is to be expected that the autocorrelation analysis will give a more suitable description. Attempts of this kind of analysis have already been made by Stevens (ref. 1).

The autocorrelation function  $\Phi(\tau)$  of a time process  $f(t)$  is defined by

$$\Phi(\tau) = \lim_{T \rightarrow \infty} \frac{1}{2T} \int_{-T}^{+T} f(t) f(t \pm \tau) dt \quad (1)$$

\*"Untersuchung unperiodischer Zeitvorgänge mit der Autokorrelations- und der Fourieranalyse." Acustica, Bd. 4, Nr. 3, 1954, pp. 365-379.

where  $f(t \pm \tau)$  is the time function for an earlier and later time instant  $\tau$ , respectively. The autocorrelation function is, thus, a simplified form of the time function in which all phase relations are neglected, and is related to the original time function in the same way that the power spectrum  $|\bar{A}(\nu)|^2$  is related to the spectral function  $\bar{A}(\nu)$  (in magnitude and phase).

According to Wiener, who introduced the autocorrelation function in information theory,<sup>1</sup> the theorem, named for him, holds that the power spectrum and the autocorrelation function of a time function form a pair of Fourier transforms. Fundamentally, it is thus not to be expected that the autocorrelation analysis should yield more than the Fourier analysis. However, in any individual case, the investigation of a time function according to either method of analysis may be more advantageous.

The autocorrelation analysis offers an advantage, for example, in the analysis of statistical processes for which only the probability distribution is known (ref. 3). These processes are not directly accessible to the theoretical treatment with the Fourier analysis, whereas, with the aid of the ergodic hypothesis (equality of the ensemble and time average of a statistical process), the autocorrelation function can be directly computed from the probability distribution. From this function and through a Fourier transformation, the frequency spectrum of the statistical process is obtained. This property of the autocorrelation function as a mediator between the probability distribution and the frequency spectrum of a statistical noise is not applied, however, in the present work.

Since the autocorrelation analysis of time functions represents a somewhat unfamiliar mode of treatment, it appears suitable first to measure the autocorrelation functions of simple noises and compare them with the measured Fourier spectra before we begin to analyze complex noises (e.g., sibilant consonants). The present investigations are correspondingly divided into the following four groups:

- (A) Investigations on filtered noises
- (B) Investigations on frequency modulated impulses
- (C) Investigations on a noise on which a periodic component is superposed
- (D) Investigation of voiceless and voiced sibilant and fricative consonants

<sup>1</sup>A review of the properties and applications of the autocorrelation function is given in a work by Lee and Wiesner (ref. 2).

Several properties of the autocorrelation function may be stated in advance:

(a) The autocorrelation function is a symmetrical function. Its maximum value lies at  $\tau = 0$ , and is equal to the time-averaged square of the time function, that is,

$$\Phi(0) = \overline{f^2(t)} \quad (2)$$

(b) The autocorrelation function of a sine or cosine function is a cosine function of equal period. The autocorrelation function of a statistical noise is an exponential function which drops more rapidly as the noise frequencies become higher. In general, it can be stated that the wider the frequency band of a time function the more rapidly its autocorrelation function drops with increasing  $\tau$ .

(c) If the noise contains various periodic and aperiodic components, each one begins at  $\tau = 0$  with its maximum value and then, depending on its frequency-band width, drops more or less rapidly, independently of the other components. In this way periodic components, for example, can be sifted out of an aperiodic noise. For  $\tau = 0$ , the energy contribution  $f^2(t)$  of each component can be observed.

(d) The curvature of the autocorrelation function at the zero crossing is connected with the mean number  $\overline{\rho}_0$  of the zero crossings per second of the initial function:

$$\overline{\rho}_0 = k_0 \sqrt{\frac{-\Phi^{II}(0)}{\Phi(0)}}, \quad k_0 \approx \frac{1}{\pi} \quad (3)$$

(see refs. 4 and 5).

(e) For the mean number of maxima and minima per second of the time function the following expression applies:

$$\overline{\rho}_m = k_m \sqrt{\frac{\Phi^{IV}(0)}{-\Phi^{II}(0)}}, \quad k_m \approx \frac{1}{\pi} \quad (4)$$

## 2. COMPUTATION OF THE AUTOCORRELATION FUNCTION OF A FILTERED NOISE

The autocorrelation function of the filtered noise can be computed by two different methods (refs. 3 and 5). The first method makes use of the definition of the autocorrelation function (eq. (1)), and the second method makes use of Wiener's theorem.

4191

CM-1 back

(a) The time function, which is to be correlated with itself, is the received function of the filter if the filter is excited by a statistical noise with constant spectral amplitude (white noise). This noise can also be regarded as a statistical, infinitely dense, sequence of  $\delta$  impulses. When excitation of the filter by a single  $\delta$  impulse occurs, the received function is equal to the so-called weighting function  $W(t)$  of the filter, which is connected with its transfer function  $Y(\nu)$  through a Fourier transformation

$$W(t) = \int_{-\infty}^{+\infty} Y(\nu) e^{j2\pi\nu t} d\nu \quad (5)$$

The autocorrelation function of the output voltage is, in this case, according to equation (1):

$$\Phi(\tau) = \lim_{T \rightarrow \infty} \frac{1}{2T} \int_{-T}^{+T} W(t) W(t \pm \tau) dt \quad (6)$$

It is shown (ref. 3) that equation (6) holds true not only for the excitation of the filter by a single  $\delta$  impulse, but also for the excitation by a statistical sequence of  $\delta$  impulses (i.e., for noises). The autocorrelation function of the filtered noise can thus be computed if the transfer function of the filter is known.

(b) The Wiener theorem represents a relation between the autocorrelation function and the spectral density of a time function.

Let the time function be  $f_T(t)$  in the region  $-T \leq t \leq +T$  and zero outside this region. Then its Fourier transform, the spectral function is

$$A_T(\nu) = \int_{-\infty}^{+\infty} f_T(t) e^{-j2\pi\nu t} dt = \int_{-T}^{+T} f(t) e^{-j2\pi\nu t} dt \quad (7)$$

The spectral density is defined as

$$G(\nu) = \lim_{T \rightarrow \infty} \frac{1}{T} |A_T(\nu)|^2 \quad (8)$$

Wiener's theorem states that

$$\Phi(\tau) = \int_0^{\infty} G(\nu) \cos 2\pi\nu\tau d\nu \quad (9)$$

that is, the autocorrelation function and the spectral density are connected by a Fourier transformation.

The spectral density of the output of a filter, whose input is a white statistical noise of spectral density  $N$ , can be computed from the transfer function

$$G(\nu) = N|Y(\nu)|^2 \quad (10)$$

For the computation of the autocorrelation function of filtered noises the following scheme is thus obtained:

$$(1) \quad \begin{array}{c} \overline{Y(\nu)} \\ W(t) \\ \underline{\Phi(\tau)} \end{array} \quad \begin{array}{c} G(\nu) \\ (2) \end{array}$$

In the first case, we go from the frequency into the time plane through Fourier transformation, and all phase relations are then eliminated; in the second case, the phases are first dispensed with in the frequency range, and then a Fourier transformation is carried out.

In the present work it is suitable to apply the first method for the RC and LC filters, and the second method for the rectangular filters.

### Examples

#### 1. RC filter

The transfer function of the RC filter is read from the circuit diagram (fig. 6(a)) as:

$$Y(\nu) = \frac{1/j2\pi\nu C}{R + 1/j2\pi\nu C} = \frac{1/RC}{j2\pi\nu + 1/RC} \quad (11)$$

The weighting function is then given by the Fourier transformation as

$$W(t) = \frac{1}{RC} e^{-t/RC} \quad (12)$$

According to equation (6), there is obtained for the autocorrelation function

$$\Phi(\tau) = \lim_{T \rightarrow \infty} \frac{1}{2T} \frac{1}{(RC)^2} \int_{-T}^{+T} (e^{-t/RC})^2 e^{-|\tau|/RC} dt \quad (13)$$

or

$$\Phi(\tau) = \Phi(0)e^{-|\tau|/RC} \quad \text{with } \Phi(0) = \overline{W^2(t)} \quad (14)$$

Similarly, there is obtained for the LC filter (fig. 7(a)),

$$Y(\nu) = \frac{1/LC}{(j2\pi\nu + \alpha)^2 + \beta^2} \quad (15)$$

$$\Phi(\tau) = \Phi(0)e^{-\alpha|\tau|} \cos \beta|\tau| \quad (16)$$

where  $\beta$  is the natural frequency of the damped circuit and in  $\alpha$  all the losses of the filter are included. The autocorrelation function is thus an exponential damped cosine function.

## 2. Rectangular filter

Transfer function:

$$\begin{aligned} Y(\nu) &= A \quad \text{for } \nu_0 - \Delta\nu/2 < \nu < \nu_0 + \Delta\nu/2 \\ Y(\nu) &= 0 \quad \text{elsewhere} \end{aligned} \quad (17)$$

The spectral density of the filtered noise, according to equation (10) is

$$G(\nu) = NA^2 \quad \text{in the transmission region} \quad (18)$$

and

$$G(\nu) = 0 \quad \text{elsewhere}$$

According to the Wiener theorem (eq. (9)), there is obtained for the autocorrelation function

$$\Phi(\tau) = NA^2 \int_{\nu_0 - \Delta\nu/2}^{\nu_0 + \Delta\nu/2} \cos 2\pi\nu\tau \, d\nu \quad (19)$$

$$\Phi(\tau) = \frac{NA^2}{\pi} \cos 2\pi\nu_0\tau \frac{\sin \pi\Delta\nu\tau}{\tau} \quad (20)$$

The autocorrelation function of the rectangular filter is a cosine function whose amplitude does not decrease exponentially but decreases like a slit function.

For the rectangularly bounded low pass filter with the limiting frequency  $\nu_{gr}$  there holds, with  $\Delta\nu = 2\nu_0 = \nu_{gr}$

$$\Phi(\tau) = \frac{NA^2}{2\pi} \frac{\sin 2\pi\nu_{gr}\tau}{\tau} \quad (21)$$

### 3. APPARATUS

#### (A) Autocorrelator

An apparatus was developed which made it possible, from a given time function  $f(t)$ , to determine the autocorrelation function according to equation (1). The block diagram of the apparatus is shown in figure 1.

The values of the time function were recorded on an endless magnetic tape, about 1 meter in length, which could receive speech up to 95 percent of its length. The interval between recordings was determined by the distance of the erase head from the record head. The frequency-response curve of the magnetic tape is seen in figure 2, where the ordinate has a linear scale. This record was obtained by recording a very broad banded noise on the magnetic tape, and analyzing the played back noise with a wide-range spectrum analyzer (ref. 7). The response is uniform up to about 16 kilocycles per second, and then drops rapidly. In measurements with pure tones and for the noise investigations, the time function was directly obtained without using a storage from the vibrating buzzer or the noise generator.

A properly terminated lumped-constant transmission line was employed as a delay mechanism. The characteristics of the transmission line were:  $C = 48,900$  micromicrofarads and  $L = 5.99$  millihenries, from which a characteristic impedance of  $Z = 350$  ohms and a time delay per section  $\tau_0 = 17.2$  microseconds, was obtained. The measured limiting frequency was 25 kilocycles. The damping of the transmission line for 50 sections, giving a time delay of about 850 microseconds, was 1.2 decibels at 2000 cycles per second, and up to 1.5 decibels for higher frequencies. In order to equalize the frequency dependence produced by passing the signal through the delay line, the undelayed voltage was conducted through several sections of delay line having an equal impedance; in addition, negative delays could then also be realized. At a maximum, the time function could be delayed by 2.5 milliseconds and by -0.014 millisecond.

Multiplication. - Most of the multiplication procedures that have become familiar are eliminated when the following requirements are set:



- (1) The product should be zero if a factor becomes zero (e.g., not satisfied in multiplicative mixture with a hexode).
- (2) A true four-quadrant multiplication should be carried out, that is, the sign of the two factors should be taken into account (not satisfied in the case of all logarithmic and impulse modulation processes).
- (3) The multiplier should not simultaneously integrate with a fixed time constant (not satisfied, e.g., with dynamometers, electrometers, and thermoconverters).
- (4) The frequency response of the multiplier must be from about 50 cycles per second to 15 kilocycles per second.
- (5) Independence of the multiplication on the input voltages of the multiplier (not satisfied when operating in the quadratic region of tube characteristic curves).

All the preceding requirements are satisfied, in a very simple manner, by a ring modulator whose four rectifier elements have very accurate equal characteristic curves. Elements corresponding to each other were selected from a large number of rectifiers.<sup>2</sup> The curve in figure 3, which simultaneously represents the characteristic of the entire autocorrelator, shows that the product voltage  $\Phi(0)$  is within a wide range proportional to the product of the two (in this case equal) input voltages  $f^2(t)$ . Using this measurement, the modulation of the multiplier is 30 millivolts. For larger modulation, the product  $\Phi(0)$  indicated is too small. Small asymmetries of the rectifier can largely be equalized by reversing the poles of one of the two voltages on the multiplier, and then taking their average. The integration was carried out with an RC element whose time constant could be readily varied. Generally, a time constant  $RC = 50$  milliseconds ( $R = 5k\Omega$ ,  $C = 10\mu F$ ) was used. In these measurements, therefore, we are dealing with an autocorrelation with limited integrating time (i.e., a short-time autocorrelation) (ref. 6).

Indicator mechanism. - The very small direct voltage delivered by the integrator is proportional to the autocorrelation function, and can be directly measured with a very sensitive galvanometer. In order to circumvent the inconvenient galvanometer measurement and make it possible to register the measurement results automatically, the direct voltage was broken up with a relay to the beat of the net power supply frequency. From the resulting rectangular voltages the fundamental frequency was filtered out with an octave band width filter. After corresponding amplification, this alternating voltage was conducted to a cathode-ray oscillograph on whose screen, and on synchronization of the time deflection with the supply frequency, it was possible to read the autocorrelation function in magnitude and sign. Because of the greater reading

<sup>2</sup>The multiplier was set up by S. Vogel.

accuracy, however, the magnitude of  $\Phi(\tau)$  was generally read on an indicator instrument connected with the measuring amplifier.

### Testing of Autocorrelator

#### 1. Frequency Dependence

The frequency dependence of the entire autocorrelation apparatus (without the storage magnetic tape) is shown in figure 4. The response is flat up to about 10 kilocycles per second. The waviness at the higher frequencies is due to the delay circuits, whose wave resistance is no longer constant in the neighborhood of the limiting frequency.

#### 2. Autocorrelation of a Sine Oscillation

The continuous curve in figure 5 shows the computed autocorrelation function of a sine oscillation of 1940 cycles per second; the points shown are the measured values. The agreement for small  $\tau$  is very good; for large  $\tau$  the damping of the delay circuit becomes appreciable, for which however, a correction can be made if the measured values are plotted on a logarithmic scale.

#### 3. Autocorrelation of a Periodically Interrupted Time Function

Since for all speech investigations the time function was periodically interrupted because of the gaps on the magnetic tape, it was ascertained, with the aid of a sine function impressed on the tape, that the apparatus also operated reliably in this case.

### (B) SOUND ANALYZER

For the sound analysis, the wide-range spectrum analyzer of Tamm and Pritsching (ref. 7) was applied. It contained a mechanical filter of 15 cycles per second band width and a very sharp cutoff. The analysis time amounted to 150 seconds for the frequency range of 0 to 20 kilocycles per second.

### (C) DECIMAL COUNTER

To determine the zero crossings of the time functions, an electronic decimal counter was employed.<sup>3</sup> In this apparatus, for each zero crossing of the input voltage, an impulse is released by a trigger and is counted

<sup>3</sup>Developed in the III. Physical Institute of the University of Göttingen by H. Henze.

in the usual manner by the multivibrator principle. The apparatus can count about  $2 \times 10^6$  zero crossings per second in a uniform series of crossings and, therefore, possesses a time-resolving power of  $0.5 \times 10^{-6}$  second. This resolving power is also sufficient to take care of the irregular sequence of zero crossings of a statistical noise exactly, providing a frequency range of 20 kilocycles per second is not essentially exceeded.

In statistical processes, the measured number of zero crossings is somewhat dependent on the input voltage of the counter. If the maximum between two neighboring crossings is so small that the trigger does not respond, only one impulse is released. On the other hand, for very large input voltages, the counter can be blocked for a short time so that too few zero crossings are indicated. For these reasons, in the case of each noise, the dependence of the number of crossings on the input voltage of the counter was measured, and the measurements were considered reliable only if the indication remained constant over a large range of input voltage.

#### 4. MEASUREMENT RESULTS

##### (A) FILTERED NOISE

As a noise source, a wide band amplifier (Rohde and Schwarz), which supplied a uniform noise extending far above 20 kilocycles per second, was employed.

Two groups of filters are distinguished: (1) the usual RC and LC filters and (2) the so-called "ideal filter" whose pass band is limited (e.g., octave, one-third octave, and low-pass filters). In the case of the rectangular filters, the envelope of the autocorrelation function has the form of a slit function  $\sin \alpha\tau/\alpha\tau$ , whereas in the case of the LC filters, it is an exponential function.

For each noise the following measurements were carried out:

- ( $\alpha$ ) Measurement of the frequency response of the filter with pure tones
- ( $\beta$ ) Spectral analysis of the filtered noise with the wide-range spectrum analyzer
- ( $\gamma$ ) Autocorrelation analysis of the filtered noise
- ( $\delta$ ) Determination of the average number of zero crossings per second of the time function with the decimal counter

## 1. Noises over RC Filter

From figure 6(a),

$$R = 16 \text{ k}\Omega$$

$$C = 4.5 \times 10^{-9} \text{ F}$$

$$RC = 72 \times 10^{-6} \text{ s}$$

Spectrum curve of the noise:

$$|A(\nu)| = \sqrt{1/[1 + (\nu/\nu_{gr})^2]}, \quad \nu_{gr} = 1/2\pi RC = 2210 \text{ cps}$$

Autocorrelation function:

$$\Phi(\tau) = \Phi(0)e^{-|\tau|/RC}$$

Measurements:

( $\alpha$ ), ( $\beta$ ) The filter response curves determined with pure tones and the spectral analysis of the filtered noise, give a limiting frequency of 2220 cycles per second. At higher frequencies up to 25 kilocycles per second, there occurs the normal drop with  $1/\nu$ , while still higher frequencies are completely cut off by the delay circuit.

( $\gamma$ ) In figure 6 the measured autocorrelation curve is shown for linear and logarithmic scale. It is essentially an exponential function with a time constant  $RC = 80$  microseconds. This value corresponds to a limiting frequency of 2000 cycles per second; the deviation from the theoretical value thus amounts to about 10 percent. The reason for the flattening of the autocorrelation function at  $\tau = 0$  is that the frequencies above 25 kilocycles per second are entirely absent (see (a)). From the circle of curvature at the zero crossing there is obtained, for the average number of zero crossings, according to equation (3), a value of  $8.5 \times 10^3 \text{ sec}^{-1}$ . This number is very uncertain, since the measurements could not be carried out for a sufficiently small value of  $\tau$ .

( $\delta$ ) The counter measurement gave a value of  $6.2 \times 10^3 \text{ sec}^{-1}$  for the average number of zero crossings.

Measurement results on additional RC filters<sup>4</sup> whose time constants embraced a range of 1:50 are presented in table I.

<sup>4</sup>The author wishes to thank P. Dämmig for his help in carrying out the RC filter measurements.

## Results:

A noise that has passed through an RC filter can be conveniently analyzed with the autocorrelator. The time constant RC of the filter is, with the given apparatus, determined to about 10 percent error. It is important, however, that no phase shifts occur between the filter and the multiplier; otherwise, the autocorrelation curve is falsified. A cutting off of the high frequencies between the filter and the multiplier evidences itself in the flattening of the autocorrelation curve at the point  $\tau = 0$ , rather than possessing a finite slope at this point.

## 2. Noise Through LC Filter (fig. 7(a)) with Various Amounts of Damping

$$L = 4.9 \text{ henries}$$

$$C = 630 \text{ micromicrofarads}$$

$$\nu_0 = 2865 \text{ cycles per second}$$

The loss factor of the coil was very small ( $\eta_{OL} = R_r/2\pi\nu_0 L = 0.06$ ). The loss factor of the condenser was varied by parallel connecting of resistances  $R_p$  ( $\eta_{OC} = 1/R_p 2\pi\nu_0 C = 0.22$ ;  $0.44$ ; and  $1.10$ ). The frequency curve of the noise is

$$|A(\nu)| = \sqrt{\frac{1}{[1 - (2\pi\nu)^2 LC + R_r/R_p]^2 + (2\pi\nu)^2 LC(\eta_{OL} + \eta_{OC})^2}}$$

and possesses, as is obtained through differentiation, a maximum at  $\nu_r$ , the resonance frequency of the filter:

$$\nu_r = \nu_0 \sqrt{1 - \frac{1}{2}(\eta_{OL}^2 + \eta_{OC}^2)}$$

The autocorrelation function is

$$\Phi(\tau) = \Phi(0)e^{-\alpha|\tau|} \cos \beta|\tau|$$

where

$$\alpha = \frac{1}{2} \left( \frac{R_r}{L} + \frac{1}{R_p C} \right)$$

$$\beta^2 = \frac{1}{LC} - \frac{1}{4} \left( \frac{R_r}{L} - \frac{1}{R_p C} \right)^2$$

$\beta = 2\pi\nu_f$  is the angular frequency of the free damped oscillations of the filter. The frequency

$$\nu_f = \nu_0 \sqrt{1 - \frac{1}{4} (\eta_{OL} - \eta_{OC})^2}$$

agrees with the resonance frequency  $\nu_r$  only in the case of very small damping.

For the average number of zero crossings per second of the filtered noise there is obtained, according to equation (3)

$$n = \frac{1}{\pi} \sqrt{\frac{-\Phi''(0)}{\Phi(0)}} = 2\nu_r$$

Measurements:

$$R_p = 400 \text{ k}\Omega$$

$$\eta_{OC} = 0.22$$

The over-all loss factor of the filter is

$$\eta_0 = 0.22 + 0.06 = 0.28$$

( $\alpha$ ) From the filter response curve measured with pure tones (fig. 7(a)) there is obtained a resonance frequency  $\nu_r = 2820$  cycles per second (theoretical value 2820 cps), and a half-value width  $\Delta\nu = 870$  cycles per second. The measured loss factor is thus  $\eta_0 = 0.30$ .

( $\beta$ ) The spectrum (fig. 7(b)) of the filtered noise shows the same picture; however, the resonance frequency and the half-value width cannot be read with the same accuracy as in the filter measurement with pure tones.

( $\gamma$ ) From the measured autocorrelation function (fig. 7(c)) there is obtained a frequency of 2740 cycles per second (theoretical value 2850 cps), and a damping  $\eta = \ln \Phi(0) / (\pi \ln \Phi_{\max} 1) = 0.28$  (theoretical value likewise  $\eta_0 = 0.28$ ). The damping of the transmission line is taken into account. The determination of the zero crossings of the time function from the radius of curvature of the autocorrelation function at  $\tau = 0$  is very inaccurate. There is obtained approximately  $n = 4000 \text{ sec}^{-1}$ .

( $\delta$ ) The determination of the number of zero crossings per second with the decimal counter gave  $n = 5050 \pm 60$ , or expressed as a frequency,  $\nu = 2525 \pm 30$  cycles per second (theoretical value, 2820 cps).

Measurements for another loss factor of the LC filter are presented in figure 8. It is clearly seen in what manner the spectrum curve and the autocorrelation curve depend on each other. The wider the frequency curve, the more damped is the autocorrelation function.

Table II lists all the experimental results that were obtained with LC filters of different damping and serves for quantitatively comparing the individual measuring methods. This table also shows that the natural frequency and damping of LC filters may be determined with the given autocorrelator within about 15-percent error. Only for the most strongly damped filter,  $\eta_0 = 1.2$ , do larger deviations occur. This was found to be true for all filters whose frequency range reaches to very low frequencies and is evidently due to the phase shifts within the amplifier at very low frequencies.

### 3. Noise Through Rectangular Filter

Frequency response curve of the filter:

$$Y(\nu) = A \quad \text{for} \quad \nu_0 - \Delta\nu/2 < \nu < \nu_0 + \Delta\nu/2$$

and

$$Y(\nu) = 0 \quad \text{elsewhere}$$

If  $N$  is the constant spectral density of the noise, then

$$\left. \begin{aligned} G(\nu) &= N|Y(\nu)|^2 = NA^2 \quad \text{for} \quad \nu_0 - \Delta\nu/2 < \nu < \nu_0 + \Delta\nu/2 \\ G(\nu) &= 0 \quad \text{elsewhere} \end{aligned} \right\}$$

The autocorrelation function, according to equation (20), is

$$R(\tau) = \frac{NA^2}{\pi\tau} \cos 2\pi\nu_0\tau \sin \pi\Delta\nu\tau$$

The following three filters were investigated:

(a) Octave filter  $\nu_0 = 4800$  cps,  $\Delta\nu = 3200$  cps

(b) One-third octave filter  $\nu_0 = 2850$  cps,  $\Delta\nu = 700$  cps

(c) Low pass filter  $\nu_{gr} = 2\nu_0 = \Delta\nu = 16$  kcps

## (a) Noise through octave filter

(α) Figure 9(a) shows the frequency response curve of the filter measured with sine tones. To determine the half-value frequencies 6305 and 3100 cycles per second, the decimal counter was used as a frequency meter. There was obtained  $\nu_0 = 4702$  cycles per second and  $\Delta\nu = 3205$  cycles per second.

(β) The spectral analysis of the noise is shown in figure 9(b). The frequency response curve of the filter is also well reproduced in this manner.

(γ) The continuous curve in figure 9(c) is computed from formula (20) for  $\nu_0 = 4800$  cycles per second and  $\Delta\nu = 3200$  cycles per second. The measured points (the crosses indicate  $-\tau$  and the circles indicate  $+\tau$ ) agree quite well with the computed curve. As a measure for the damping of the autocorrelation curve, the ratio of the first maximum to the first minimum may be used. For an octave filter, there is theoretically obtained  $\Phi(0)/\Phi_{\min} = 1.2$ ; the measured value was  $\Phi(0)/\Phi_{\min} = 1.3$ . From the radius of curvature at the zero crossing, there is computed a mean number of zero crossings of  $10.8 \times 10^3 \text{ sec}^{-1}$ , corresponding to a frequency of 5400 cycles per second. The determination of the radius of curvature is not very accurate, however.

(δ) The counting of the zero crossings with the decimal counter gave  $n = (10.0 \pm 0.2) \times 10^3$ , that is,  $\nu = 5.0 \pm 0.1$  kilocycles per second. The comparison with the theoretically predicted value

$$n = 2 \sqrt{\frac{\nu_b^3 - \nu_a^3}{3(\nu_b - \nu_a)}} = 9.8 \times 10^3 \text{ sec}^{-1}, \quad \begin{aligned} \nu_b &= \nu_0 + \Delta\nu/2 \\ \nu_a &= \nu_0 - \Delta\nu/2 \end{aligned}$$

shows good agreement.

## (b) Noise through one-third octave filter

(α), (β) The response and spectrum for the one-third-octave filter show (figs. 10(a) and (b)) that although the cutoff of the filter was sharp, its top was rounded. With the decimal counter the frequencies of the half-value points were determined as 3230 and 2500 cycles per second. From this there is obtained a mean frequency  $\nu_0 = 2865$  cycles per second, and a band width  $\Delta\nu = 730$  cycles per second (theoretical values 2850 and 700 cps).

(γ) The continuous curve in figure 10(c) represents the measured autocorrelation curve. It drops somewhat more rapidly than the ideal computed autocorrelation function for a rectangular filter in figure



10(a), the maxima and minima of which are plotted as crosses in figure 10(c) (the damping of the transmission line was taken into account). For comparison, the extreme values of the autocorrelation curves for a resonance circuit of equal mean frequency and half-value width are indicated by triangles. The curve drops considerably more rapidly than the measured autocorrelation function of the third filter.

(5) With the decimal counter, a mean number of zero crossings of  $n = 5690 \pm 30 \text{ sec}^{-1}$  was measured; this corresponds to a frequency of  $2845 \pm 15$  cycles per second. If the values measured under (a) of  $\nu_0 = 2865$  cycles per second and  $\Delta\nu = 730$  cycles per second are used as a basis, then the expected value is  $n = 5.80 \times 10^3 \text{ sec}^{-1}$ . Therefore, the agreement is good.

(c) Noise over low pass

$$\text{Autocorrelation function: } \phi(\tau) = \frac{A^2}{2\pi\tau} \sin 2\pi\nu_{gr}\tau$$

As a low pass filter there was used the storage magnetic tape, whose response curve at 16 kilocycles per second drops with considerable steepness (see fig. 2).

(r) The continuous curve in figure 11 is the computed autocorrelation function for a low pass filter with a limiting frequency of 16 kilocycles per second, with which the measured points, plotted as circles, show quite good agreement.

(5) For the number of zero crossings the measurement with the counter gave  $n = 18 \times 10^3 \text{ sec}^{-1}$ . The expected theoretical value would be  $n = 1.155 \nu_{gr} = 18.5 \times 10^3 \text{ sec}^{-1}$ , a value that agrees very well with the measured value.

#### 4. Cross Correlation

Whereas the autocorrelation of a filtered noise, according to equation (6), gives the simplified weighting function of the filter (without considering the phases), the weighting function itself is obtained if a cross correlation of the output voltage of the filter with its input voltage is taken. The cross correlation makes higher demands on the apparatus since it requires two accurately equal amplifiers whose phase shift also remains small for low frequencies.

Cross-correlation curves for an RC filter ( $RC = 0.9 \times 10^{-3} \text{ sec}$ ) and for an LC filter ( $\nu_r = 1500 \text{ cps}$ ) are shown in figures 12 and 13. In contrast to the autocorrelation curves, which always start with their maximum value, the cross-correlation curves start with zero and, in

addition to the decay process, also show the starting oscillations of the filter.

### (B) POSITION MODULATED IMPULSE SEQUENCE

As an example of a process very rich in overtones, impulse sequences were investigated. The impulses were taken from the decimal counter and could be released either periodically (through a sine voltage), or in an irregular sequence (through wabbling or noise voltage). Figure 14 shows the form of the impulses at the inlet of the multiplier; they could not be made arbitrarily narrow because the transmission line limited the frequency range at 25 kilocycles per second.

The effects which the sequence of the impulses has on the autocorrelation function and on the Fourier spectrum are shown by the measurements presented in figures 15 and 16, respectively.

In (a), the impulses are released by a sine voltage of 1425 cycles per second (i.e., purely periodic). The sound analysis (fig. 16(a)), gives a spectrum of discrete partial tones, and the overtones of the impulse give a sequence of frequencies  $\nu_1$ . The autocorrelation function (fig. 15(a)), consists of individual jags which repeat periodically after the displacement time  $\tau = 1/\nu_1$ . The decrease in size of the jags with increasing  $\tau$  is a measure of the accuracy with which the sequence of impulse frequencies is controlled. In regular sequences of impulses all the peaks should be of equal height; the decrease of the maximum in figure 15(a) is due to the damping of the transmission line. A comparison with figure 14 shows that the autocorrelation function has very great similarity to the time function.

In the releasing of the impulses through a wobble tone (1400±30 cps), the autocorrelation function changes very little; the jags decrease somewhat more rapidly with increasing  $\tau$  compared with those shown in figure 15(a). The spectral analysis (fig. 16(b)) also contains the uneven partial tones which are drawn into narrow frequency bands.

If the impulses are released through a statistical process (using a noise-band width of  $\Delta\nu/\nu = 0.6$  so adjusted that the mean frequency of the impulse sequence was about 1380 cps), the jags of higher order in the autocorrelation function (fig. 15(b)), disappear. From about  $\tau = 400$  microseconds on,  $\Phi(\tau) \approx 0$ . The spectral analysis figure 16(c) shows (in place of the discrete partial tones), a wide continuous frequency band starting at about the mean frequency of the impulse sequence and decreasing very slowly after higher frequencies.

In summary, it may be said, in regard to the autocorrelation function of impulse sequences, that the decrease of the autocorrelation function at  $\tau = 0$  is determined by the content of the time function in high frequencies independently of the circumstance, whether it is a question of discrete overtones or wide frequency bands. In order to determine whether the time function is for a periodic or an aperiodic process, the autocorrelation function must be investigated up to relatively large values of  $\tau$ . Only if the autocorrelation function remains continually zero from a definite value of  $\tau$  onward does the time function correspond to an aperiodic process.

### (C) ADDITIVE SUPERPOSITION OF A PERIODIC AND AN APERIODIC TIME PROCESS

Since, in the case of language sounds, for example, voiced consonants, we are frequently dealing with a superposition of two or more time processes, it will be shown in a further model test, how the individual components can be separated with the aid of the autocorrelation analysis.

The simplest and clearest case is that of the additive superposition of a pure sine tone  $f_s(t)$  with a wide band noise  $f_r(t)$ . The autocorrelation function in this case is (ref. 2)

$$\begin{aligned}\Phi(\tau) &= \lim_{T \rightarrow \infty} \int_{-T}^{+T} [f_s(t) + f_r(t)] [f_s(t \pm \tau) + f_r(t \pm \tau)] dt \\ &= \Phi_{ss}(\tau) + \Phi_{rr}(\tau) + \Phi_{sr}(\tau) + \Phi_{rs}(\tau)\end{aligned}$$

The two terms with mixed indices drop away because the cross correlation of two incoherent processes is zero. The autocorrelation of the sum of two incoherent processes is, thus, equal to the sum of their autocorrelation functions. For the particular case  $\tau = 0$ , we have

$$\Phi(0) = \Phi_{ss}(0) + \Phi_{rr}(0) = \overline{f_s^2(t)} + \overline{f_r^2(t)}$$

that is, for  $\tau = 0$ , it is possible to obtain the square mean of the time functions from the autocorrelation diagram.

As an example, figures 17(a) and (b) show the frequency spectrum and the autocorrelation function of a mixture of noise, and a sine tone of about 4 kilocycles per second. Both noises were so adjusted that they each produced the same deflection on a tube voltmeter with linear rectification. According to Beranek (ref. 8), the mean square values are then in the ratio

$$\overline{f_r^2(t)} / \overline{f_s^2(t)} = 1.3$$

From the autocorrelation diagram, there can immediately be read the energy ratio

$$\frac{\Phi_r(0)}{\Phi_s(0)} = \frac{\overline{f_r^2(t)}}{\overline{f_s^2(t)}} = \frac{74 - 31}{31} = 1.4$$

In order to compute the sine and noise components of the frequency spectrum, the filter width of the sound analyzer and the band width of the noise must be known; in the case considered they are 15 cycles per second and 16 kilocycles per second, respectively. From figure 17(a) there is then obtained

$$\overline{f_r^2(t)} / \overline{f_s^2(t)} = 1.5$$

In a second measurement, in which the energy of the sine tone was only one-fourth of the energy of the noise, the following values were obtained for the ratio of the two energies: theoretical value, 5.0; autocorrelation analysis, 4.8; and sound analysis, also 4.8. The accuracy of the measurement is about equal for both processes.

In the case of voiceless consonants we have to deal not with the superposition of a pure sine tone and a very broad banded noise, but frequently with the superposition of two relatively narrow but continuous frequency bands. As an example, the results are given for the voiceless "s", whose spectral analysis is shown in figure 18(a), and whose autocorrelation function is shown in figure 18(b). If it is desired to determine, from the frequency spectrum, what part of the total energy corresponds to the small peak at 7 kilocycles per second and what part of the total energy corresponds to the broad frequency range at 9 kilocycles per second, the areas under these peaks must be measured with an integrating planimeter. This measurement, which was carried out with an enlargement of figure 18(a), gave, for the ratio of the energies,  $N_9 \text{ kcps} / N_7 \text{ kcps} = 6.2$ .

The separation of the two autocorrelation functions can easily be effected if the maxima and minima of the measured autocorrelation function is plotted to logarithmic scale (fig. 18(c)). In spite of the large scatter of the measured values, two straight lines which characterize the exponential decrease of the two oscillations can easily be drawn. The steep line corresponds to the broad frequency band, and the line with smaller slope corresponds to the narrow band. From the points of intersection of the straight lines with the axis of ordinates there is read, for the ratio of the energy of the two peaks at 9 kilocycles per second to that of the narrow peak at 7 kilocycles per second:

$$\frac{\Phi_{9 \text{ kcps}}(0)}{\Phi_{7 \text{ kcps}}(0)} = \frac{90 - 14.5}{14.5} = 5.3$$

4191

OM-3 back

The agreement of the two values is satisfactory in view of the fact that the planimeter measurement is not very accurate.

#### (D) VOICED AND VOICELESS SIBILANT SOUNDS

Voiceless sibilant sounds consist of more or less broad, continuous frequency bands whose shapes depend considerably on the position of the mouth in uttering them. If, for example, the mouth is in the position for pronouncing u while the sibilant is uttered, the latter will generally contain only a single, relatively narrow frequency range.

Voiced sibilants have essentially the same frequency spectrum as the corresponding voiceless sounds except that there is, in addition, the much more energy rich, purely periodic voice tone.

According to Meyer-Eppler (ref. 9), there is defined, as a measure of the degree of voicing S of a sound, the ratio

$$S = \sqrt{\Phi_P(0)/\Phi(0)}$$

where  $\Phi_P(0)$  is the autocorrelation function of the periodic component and  $\Phi(0)$  that of the total sound, both taken for  $\tau = 0$ .

The sibilant investigated was recorded on an endless recording loop of about 1 meter length in such manner that it filled out the tape except for the unavoidable gap of 5 percent of the tape length. To determine the number of zero crossings with the counter, the gap of the recording was taken into account by counting over a longer time, measured with a stop watch (about 10 cycles of the loop) and then multiplying the indicated number of zero crossings by the factor 1.05.

In the following paragraph one example of the large number of measurements for each of the investigated sibilants (table III) will be discussed. Further, an attempt will be made to distinguish the characteristic properties of the individual sounds.

#### Voiceless Sibilants

##### 1. Voiceless "sh"

( $\alpha$ ) The spectral analysis (fig. 19(a)), gives a continuous spectrum without discrete lines. It possesses two preferred frequency ranges, a high, relatively narrow peak at 5.3 kilocycles per second (half-value width about 300 cps), and a smaller peak at 1.2 kilocycles per second.

(β) The autocorrelation curve (fig. 19(b)), has the form of a damped cosine oscillation. From the distance of the first six maxima there is obtained a period  $\tau = 185$  microseconds, corresponding to a frequency of 5.4 kilocycles per second (sound analysis 5.3 kcps). On the fundamental period is superposed a small secondary period whose value is obtained from figure 19(b) as about 740 microseconds (1.3 kcps). It corresponds to the small peak at 1 kilocycle per second in figure 19(a). To determine the half-value width of the fundamental period, the extreme values of the autocorrelation function were logarithmically plotted in figure 19(c). In spite of the considerable scatter of the measuring points (caused by the superposed secondary period), it can be seen that the points lie approximately on a straight line, and hence, that the autocorrelation function decreases exponentially and not according to the slit function  $\sin \alpha\tau/\alpha\tau$ . From this, it can be concluded that the resonator formed by the mouth cavity in speaking the "sh" sound has the properties of a simple mass-spring system, and is not a filter with rectangularly limited frequency range. The half-width value of the resonator is computed from the drop of the autocorrelation function, with account taken of the losses of the transmission line, and is found to be 360 cycles per second (spectral analysis 300 cps). The point  $\Phi(\tau = 0)$  lies uniquely above the straight line which is passed through the remaining measuring points. This fact indicates that, in addition to the preferred frequency ranges of 1.2 and 5.4 kilocycles per second, there exists a further wide noise background whose autocorrelation function drops off so rapidly that it has no effect on the remaining measuring points. In this noise background, which can also be seen on the frequency diagram (fig. 19(a)), there is contained, as can immediately be read from the autocorrelation diagram, about 35 percent of the total energy of the sibilant sound.

(γ) In the measurement with the decimal counter, there was obtained a mean number of zero crossings of  $9.8 \times 10^3 \text{ sec}^{-1}$ , corresponding to a central frequency of 4.9 kilocycles per second. This value lies about 8 percent lower than was expected according to measurements (α) and (β).

Measurements of other "sh" sounds, some of which were spoken by one person for various positions of the mouth and some by seven different persons, showed the following common properties that appear to be characteristic for the "sh" sound. The frequency spectrum often possesses two preferred frequency ranges each having a width of 500 cycles per second. The upper region generally lies between 5 and 6 kilocycles per second, the lower region between 1 and 3 kilocycles per second. Since, in uttering the "sh" sound, two cavities are formed by the position of the tongue, we are possibly dealing with the resonances of these two cavities.

## 2. Voiceless "s"

The investigations on a voiceless "s" sound (figs. 18(a), (b), and (c)), have already been discussed in the preceding section. Hence, only

the values obtained for the central frequencies and damping of the two preferred frequency ranges, according to the different methods, are collected here:

(α) Spectral analysis:

$$\nu_1 = 7.0 \text{ kcps}$$

$$\nu_2 = 8.8 \text{ kcps}$$

$$\Delta\nu_1/\nu_1 = 200 \text{ cps}$$

$$\Delta\nu_2/\nu_2 = 1500 \text{ cps}$$

(β) Autocorrelation:

$$\nu_1 = 7.4 \text{ kcps}$$

$$\nu_2 = 8.7 \text{ kcps}$$

$$\Delta\nu_1/\nu_1 = 160 \text{ cps}$$

$$\Delta\nu_2/\nu_2 = 2000 \text{ cps}$$

$\nu_2$  was computed from the distance of the first maximum of the autocorrelation diagram, and  $\nu_1$  was computed from the distance of the last of the 19 measured maxima (in fig. 18(b), only the first eight periods are drawn in).

(γ) Counter measurement: The counter, naturally, does not distinguish between the two frequencies. There were counted  $18 \times 10^3 \text{ sec}^{-1}$  zero crossings per second corresponding to a central frequency of 9 kilocycles per second. Measurements α, β, and γ are, therefore, particularly as regards the frequencies<sup>5</sup>, in good agreement with each other.

Almost all "s"-spectra (spoken by seven different speakers) have the common characteristic that frequencies below 5 and above 10 to 12 kilocycles per second, are completely absent. Between 5 and 10 kilocycles per second there is a sharply limited, very strong cleft frequency band which evidently consists of several relatively narrow frequency bands. In agreement with this, the autocorrelation diagram of "s" sounds generally has a relatively undamped character.

<sup>5</sup>The differences mentioned in section 4(A) of the characteristic frequency measured with the sound analysis and with the autocorrelation analysis, is not taken into account here.

### 3. Voiceless "f"

( $\alpha$ ) The sound analysis (fig. 20(a)) gives a very broad continuous spectrum which practically fills the entire investigated frequency range (up to 16 kcps). Individual, very narrow peaks project somewhat from the noise band.

( $\beta$ ) The autocorrelation function (fig. 20(b)) shows a section from  $0-1 \times 10^{-3}$  sec), is unusually strongly damped. At the second maximum ( $\tau = 86 \mu$  sec), the autocorrelation function amounts to only 10 percent of the value of  $\Phi(0)$ . For  $\tau > 100$  microseconds, the autocorrelation function is a very weakly damped, somewhat irregular cosine function whose period corresponds to a frequency of about 11 kilocycles per second. The waviness is not completely damped even at  $\tau = 2000$  microseconds. The jag of the spectrum to which this very undamped oscillation corresponds could not be explained. The logarithmic representation of the measured autocorrelation function showed that, in this periodic component only, about 8 percent of the total energy is contained.

( $\gamma$ ) Counter measurement: The mean number of the zero crossings amounted to  $19.6 \times 10^3$  per second, that is, the frequency center of gravity lay at about 10 kilocycles per second.

Characteristic of all investigated "f" sounds (seven different speakers) was the wide frequency band and the rapid drop of the autocorrelation function. Through suitable mouth position it was possible to stress individual frequency ranges, but the proportion of the total energy in the wide band was seldom below 75 percent.

### Voiced Sibilant Sounds

#### 4. The "zh" Sound (Voiced "sh" as in French "journal")

( $\alpha$ ) The spectrum of the voiced "zh" sound (fig. 21(a)) consists of a continuous part which is equal to the spectrum of the corresponding voiceless "sh" sound and the discrete lines of voice tone and its overtones. (The amplitude of the vocal tone is much greater than that of the noise component so that the spectrum, fig. 21(a), had to be plotted to logarithmic scale.) The voice tone lies accurately at 390 cycles per second (determined with the decimal counter), the preferred frequency ranges of the noise component at 2.5 and 6 kilocycles per second.

( $\beta$ ) Figure 21(b), represents the measured autocorrelation function, which is additively composed of three curves. In a simple manner, there can be split off a cosine curve of the period  $\tau = 26$  microseconds ( $\nu = 382$  cps), which corresponds to the voice tone ( $\Phi_s(\tau)$  in fig. 21(b)). The rest of the autocorrelation curve (fig. 21(b)) splits into a periodic



part with  $\tau = 162$  microseconds (6.2 kcps) and a noise part. The total energy is distributed, as is read from figure 21(b), as follows: voice tone, 73 percent; frequency band at 6 kilocycles per second, 5 percent; and noise part, 22 percent. The degree of voicing is

$$S = \sqrt{65/89} = 0.85$$

( $\gamma$ ) The determination of the zero crossings with the decimal counter, as in the case of all voiced sounds, is impossible here because the relatively small noise component, along with the strong voice tone, cannot be reliably determined.

#### 5. Voiced "s"

( $\alpha$ ) The sound analysis (fig. 22(a)) also shows, in addition to the discrete lines of the voice tone and its overtones, a continuous spectrum very similar to that of a voiceless "s". The preferred frequency range lies at 9 kilocycles per second, and has a half-value width of about 1.6 kilocycles per second. The frequency of the voice tone, determined with the decimal counter, was 350 cycles per second.

( $\beta$ ) The autocorrelation curve (fig. 22(b)) can very easily be split into two curves. The curve with the longer period, 3100 microseconds (322 cps), corresponds to the voice tone, whereas the other curve represents a damped cosine function of the period  $\tau = 115$  microseconds (8.7 kcps). The frequency band width computed from this oscillation is 1.5 kilocycles per second. The data of the two oscillations, computed from the autocorrelation function, thus agree very well with the results of the sound analysis. The degree of voicing of the sound can be read most simply from the autocorrelation curve

$$S = \sqrt{57/89} = 0.80$$

#### 6. Voiced "v"

( $\alpha$ ) The spectrum contains a very strong discrete line at 335 cycles per second (fig. 23(a)). The noise component is a very weak noise band that extends over the entire frequency range of the apparatus.

( $\beta$ ) The measured autocorrelation curve (fig. 23(b)) shows the same result. The voice tone has a period  $\tau = 3200$  microseconds (310 cps), and contains 96 percent of the total energy. It is superposed by a very strongly damped cosine vibration whose period is about  $\tau = 70$  microseconds (14 kcps).

Degree of voicing:

$$S = \sqrt{90/94} = 0.98$$

#### Short Sibilant Sounds

In addition to sibilant sounds, which were held for sometime, briefly uttered voiceless sibilant sounds were also investigated. The autocorrelation curves showed great similarity with those of the corresponding longer uttered sounds. Characteristic differences could not be established.

The author wishes to thank Professor E. Meyer for his suggestions and valuable advice.

#### REFERENCES

1. Stevens, K. N.: Autocorrelation Analysis of Speech Sounds. Jour. Acoustic Soc. Am., vol. 22, 1950, p. 769.
2. Lee, Y. W., and Wiesner, J. B.: Correlation Functions and Communication Applications. Electronics, vol. 23, June 1950, p. 86.
3. James H. M., Nichols, N. B., and Phillips, R. S.: Theory of Servomechanisms. Ch. 6, McGraw-Hill Book Co., Inc., 1947.
4. Chang, S. H., Pihl, G. E., and Essigmann, M. M.: Representations of Speech Sounds and Some of Their Statistical Properties. Proc. Inst. Radio Eng., vol. 39, 1951, p. 147.
5. Rice, S. O.: Mathematical Analysis of Random Noise. Bell System Tech. Jour., vol. 23, 1944, p. 282; vol. 24, 1945, p. 46.
6. Fano, R. M.: Short Time Autocorrelation Functions and Power Spectra. Jour. Acoustic Soc. Am., vol. 22, 1950, p. 546.
7. Tamm, K., and Pritsching, I.: Frequenzanalysator mit mechanischem Hochtonfilter. Acustica 1 (1951), Beiheft 1, AB 43.
8. Beranek, Leo L.: Acoustic Measurements. John Wiley & Sons, 1949, p. 453.

9. Meyer-Eppler, W.: Übersicht über die Verfahren zur Charakterisierung aleatorischer Schallvorgänge und deren Anwendbarkeit auf Geräuschlaute. Zs. Phonetik u. allgem. Sprachwissenschaft, Bd. 6, 1952, p. 269.

Translated by S. Reiss  
National Advisory Committee  
for Aeronautics

4191

TABLE I

R, Ohms	C, Farads	RC theoretical, sec	RC autocorrelation, sec	$f_{gr}$ , cps
80	$18 \times 10^{-9}$	$1.44 \times 10^{-3}$	$1.2 \times 10^{-3}$	110
50	18	.90	.8	177
30	18	.54	.5	395
15	18	.27	.3	590
15	6	.090	.086	1770
16	4.5	.072	.080	2210
15	1.9	.029	.034	5500

TABLE II

	a	Percent (a)	b	Percent	c	Percent
Resonance frequency:						
Computed	2820		2715		1810	
From filter measurement	2820	0	2510	7.5	(b)	
From counter measurement	2525	10	2305	16	2080	15
Frequency of free oscillation, $\beta/2\pi$ :						
Computed	2850		2810		2440	
From autocorrelation curve	2740	4	2460	13	1450	40
Loss factor:						
Computed	0.28		0.50		1.2	
From filter measurement	.30	7	.44	12	(b)	
From autocorrelation curve	.28	0	.42	16	2.0	70

<sup>a</sup> The percentages give the deviations of the measured values from the computed value.

<sup>b</sup> The curve is so strongly damped that neither the resonance frequency nor the half-value width could be obtained from it. The measured values, however, agree well with the computed curve (fig. 8(a)).

TABLE III

## LIST OF INVESTIGATED SIBILANTS (AND FRICATIVES)

Voiceless	Voiced
1. sh (shoe)	4. zh (as in French jour)
2. s (gas)	5. z (zone)
3. f (fine)	6. v (vine)

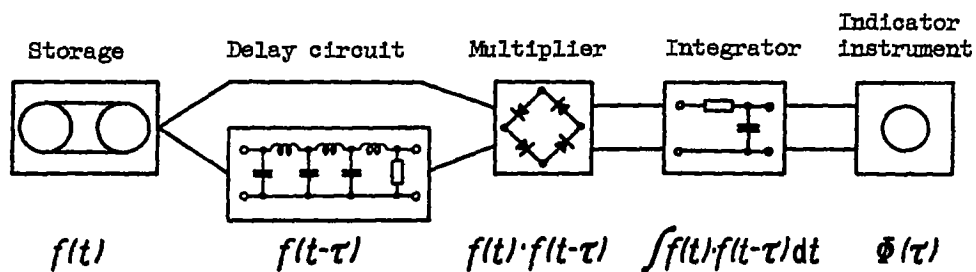


Figure 1. - Block diagram of autocorrelator.

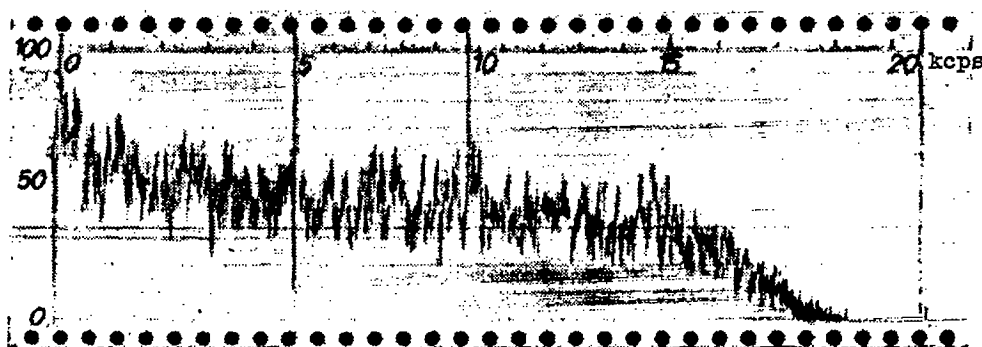


Figure 2. - Frequency curve of storage magnetic tape.

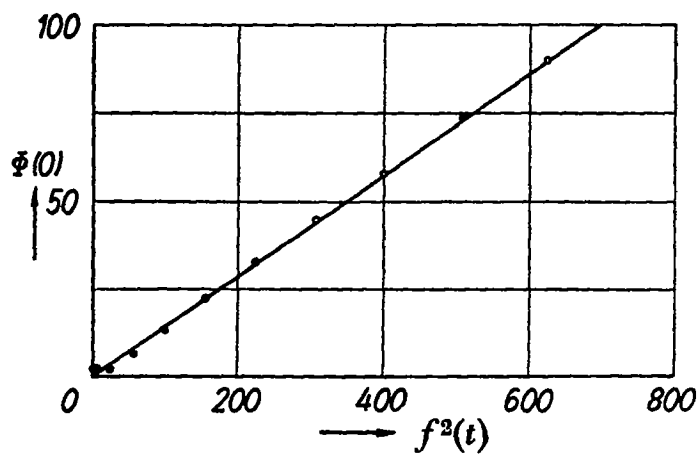


Figure 3. - Characteristic curve of over-all autocorrelation apparatus.

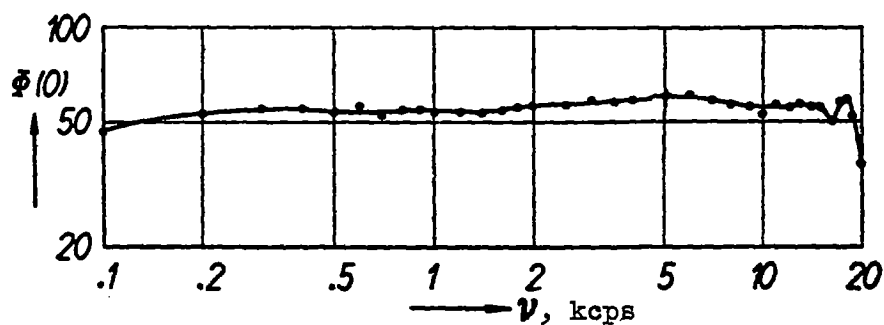


Figure 4. - Frequency response curve of autocorrelator.

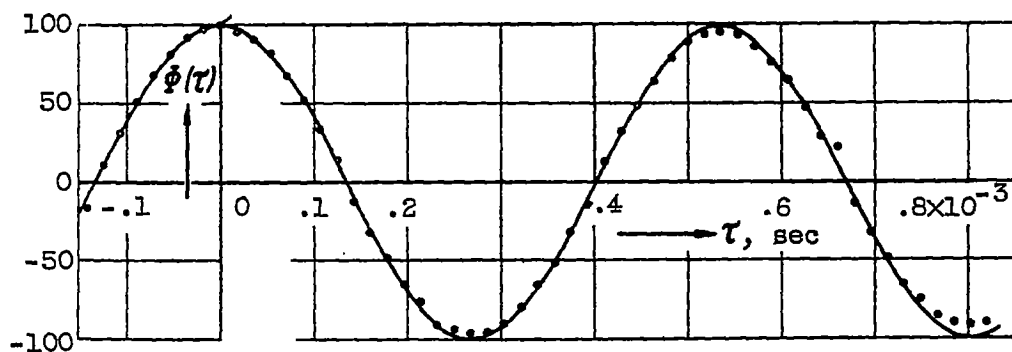
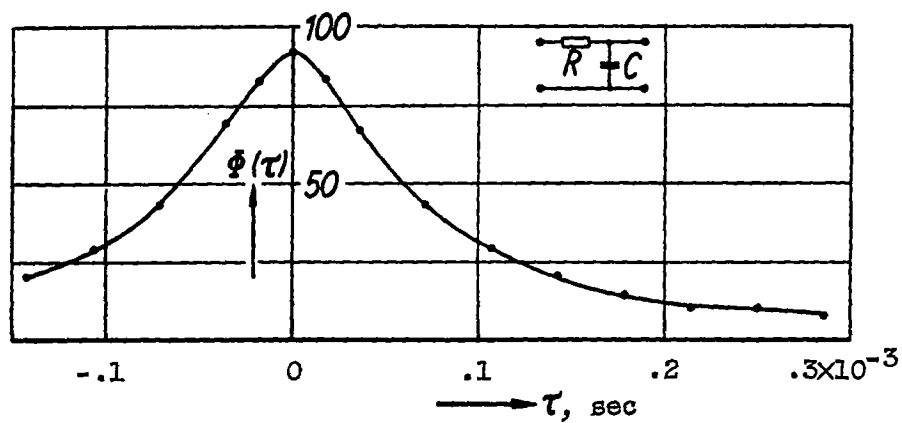
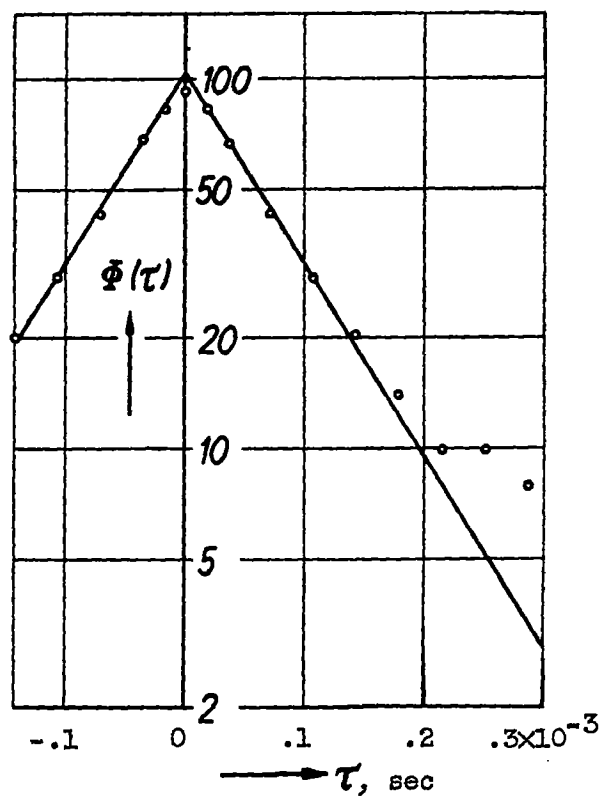


Figure 5. - Autocorrelation function of a sine function; — computed for  $\nu = 1940$  cycles per second; o o o measured.

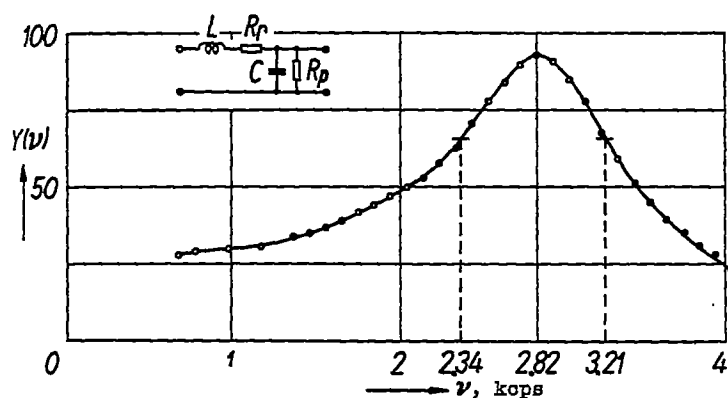


(a) Autocorrelation function in linear scale.

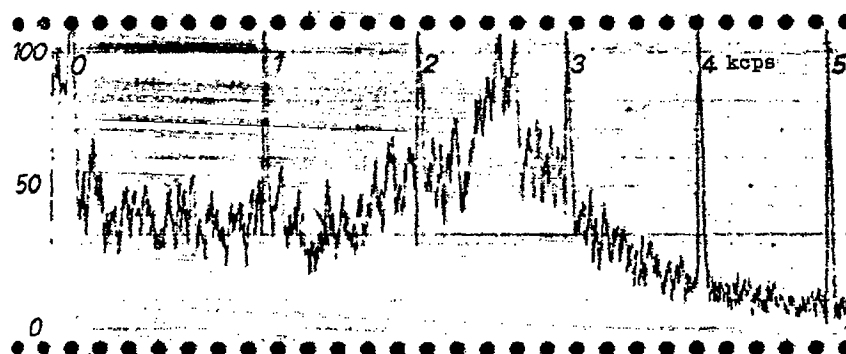


(b) Autocorrelation function in logarithmic scale.

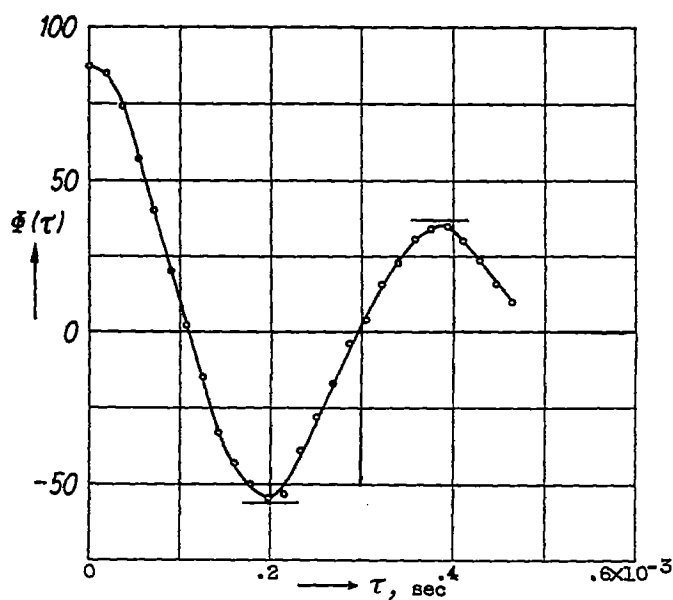
Figure 6. - Noise through RC filter.



(a) Frequency response curve of filter.



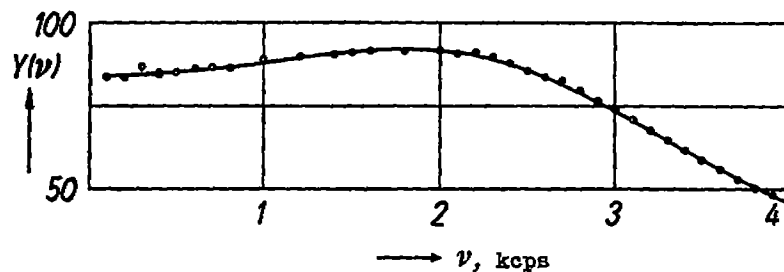
(b) Sound analysis of filtered noise.



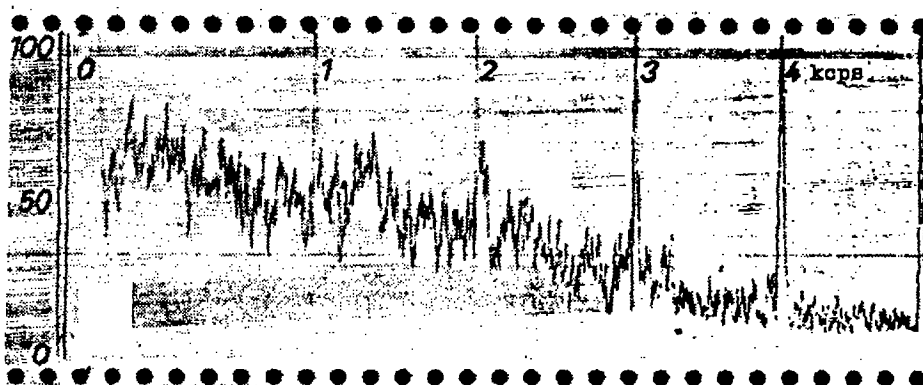
(c) Autocorrelation curve (horizontal strokes: height of maxima with account taken of delay current losses).

Figure 7. - Noise through LC filter ( $\Delta\omega/\omega_0 \approx 0.28$ ).

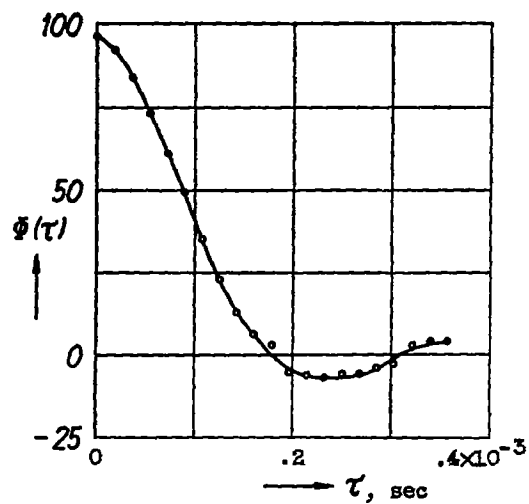




(a) Frequency response curve of filter, — computed,  
o o o measured.

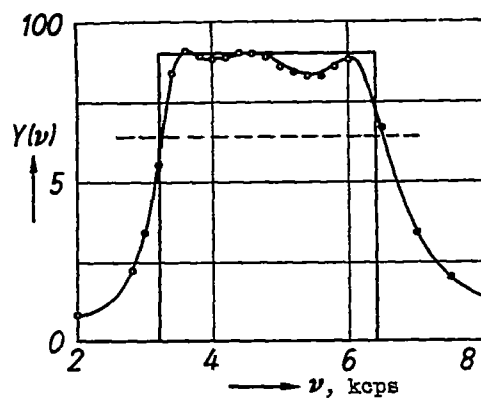


(b) Spectrum of filtered noise.

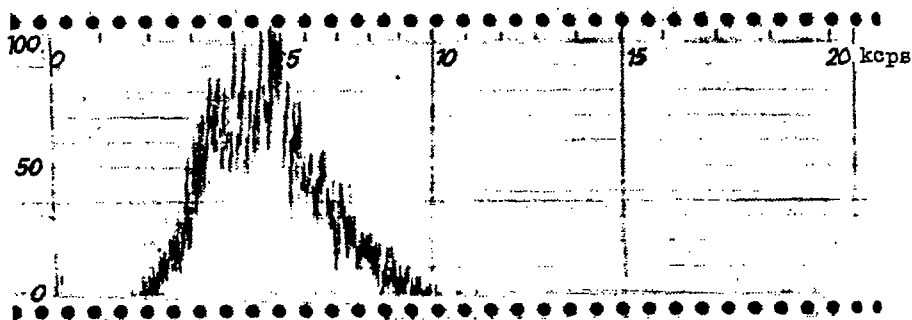


(c) Autocorrelation function.

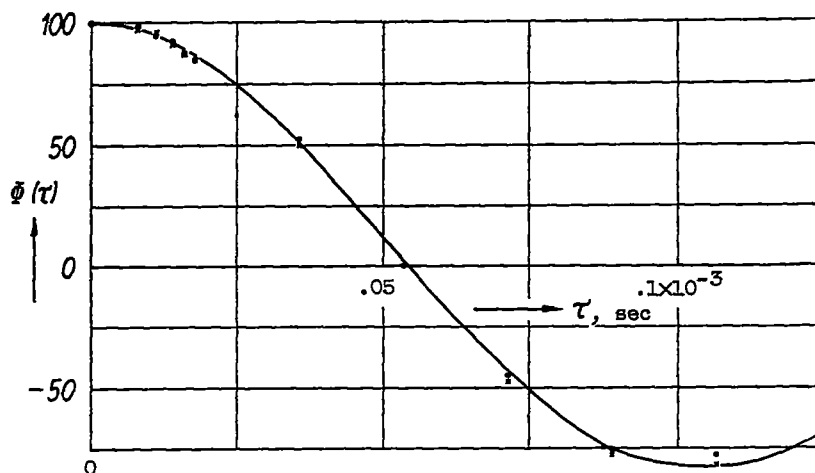
Figure 8. - Noise through LC filter  
( $\Delta v/v_0 = 1.2$ ).



(a) Frequency response curve of filter,  
 o o o measured with pure tones, —  
 simplified curve used for computing  
 autocorrelation function.

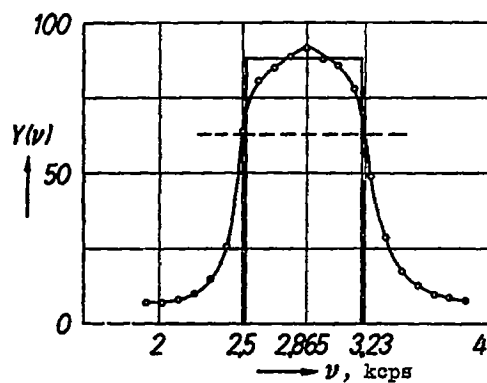


(b) Spectrum of filtered noise.

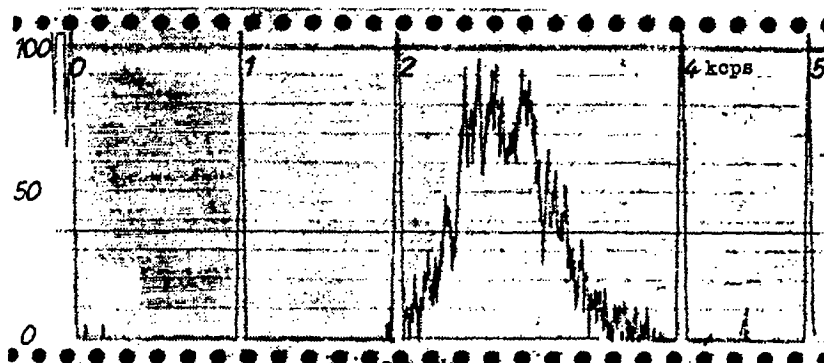


(c) Autocorrelation function; — computed from figure 9(a);  
 o o o measured for  $+\tau$ ; xxx measured for  $-\tau$ .

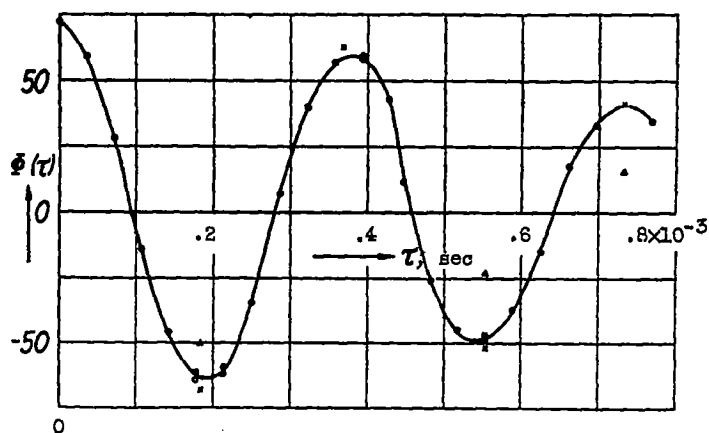
Figure 9. - Noise through rectangular filter of octave width.



(a) Frequency response curve of filter,  
 o o o measured with pure tones,  
 — simplified curve used for  
 computing autocorrelation function.



(b) Spectrum of filtered noise.



(c) Autocorrelation analysis; xx computed for rectangular filter; ΔΔ computed for resonance circle of equal frequency width; o o o measured (damping of delay circuit taken into account).

Figure 10. - Noise through rectangular filter of one-third-octave band width.

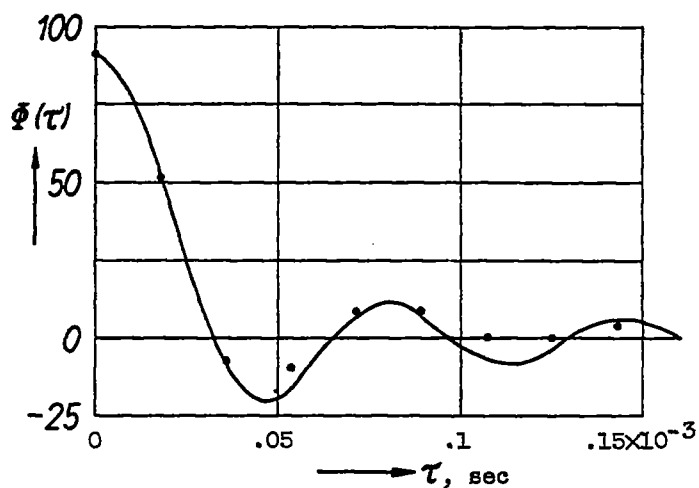


Figure 11. - Noise through low pass filter (limiting frequency 16 kcps), autocorrelation function; — computed; o o measured.

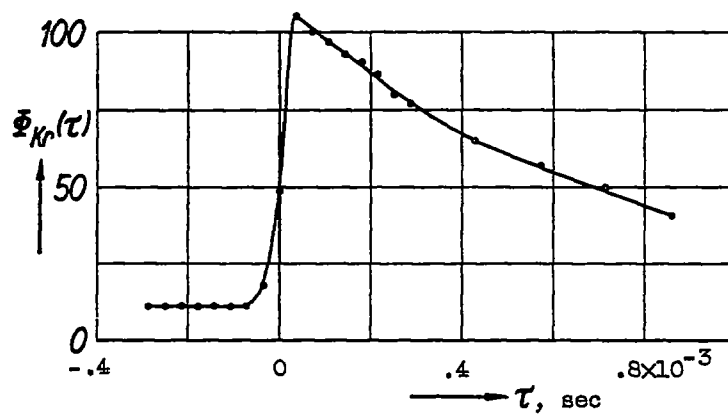


Figure 12. - Cross correlation between the input and output voltage of an RC filter ( $RC = 0.9 \times 10^{-3}$  sec).

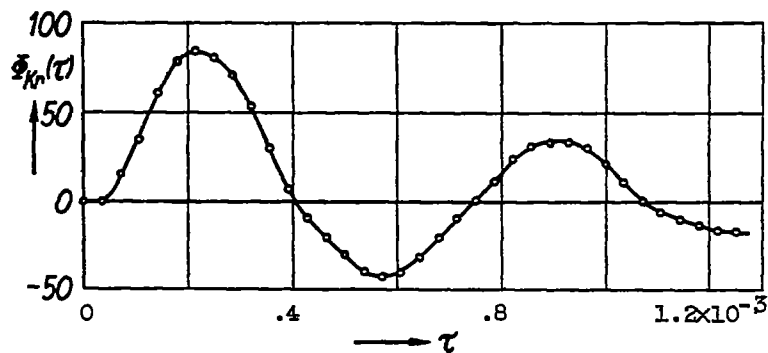


Figure 13. - Cross correlation between the input and output voltage of an LC filter ( $v_r \approx 1500$  cps).

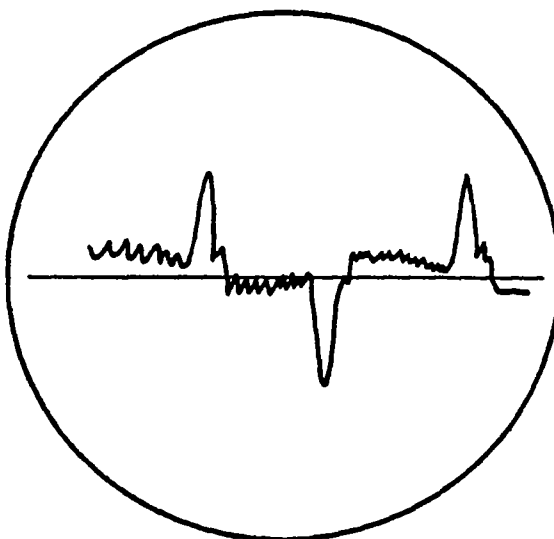


Figure 14. - Form of impulse.

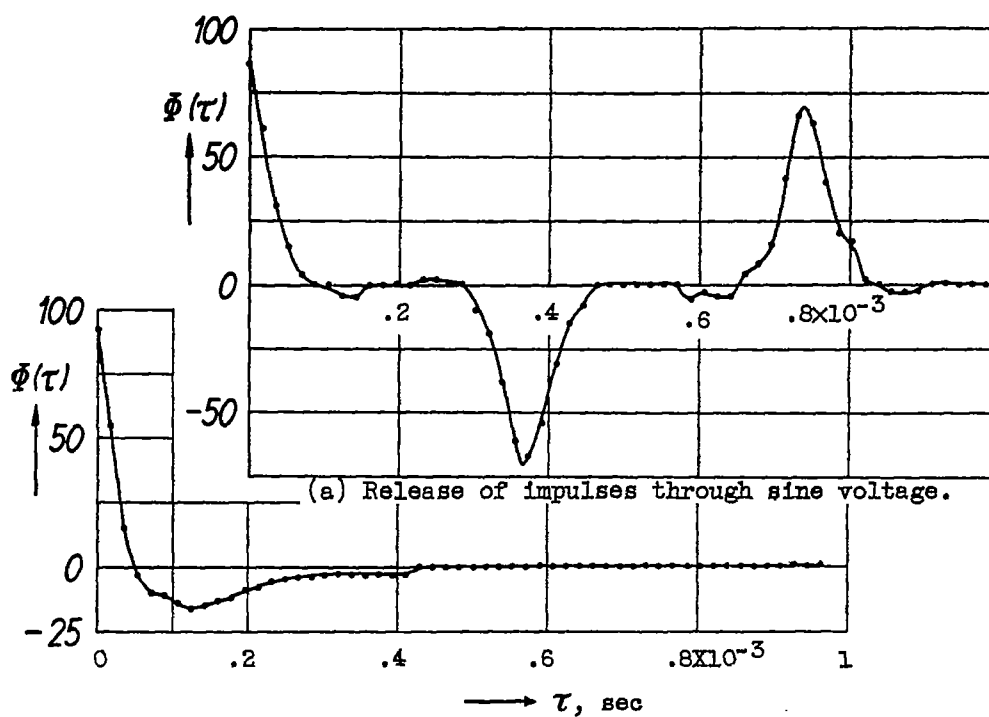
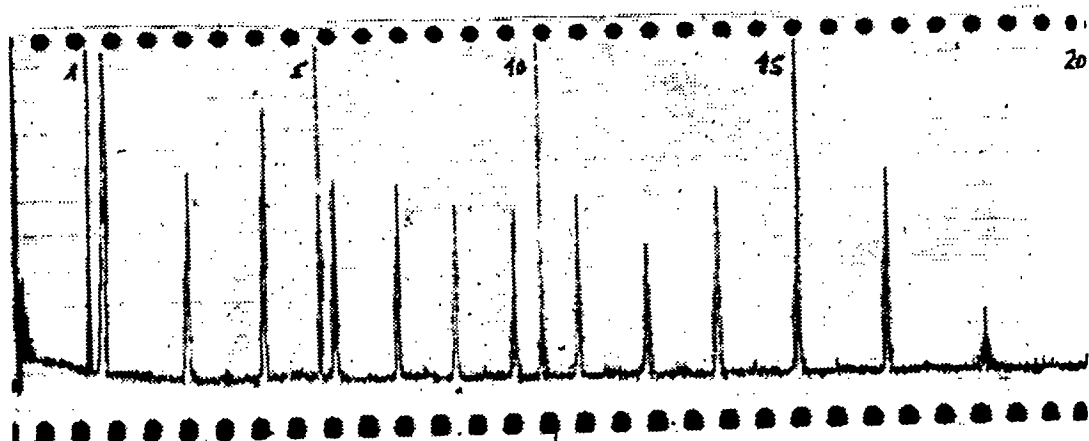
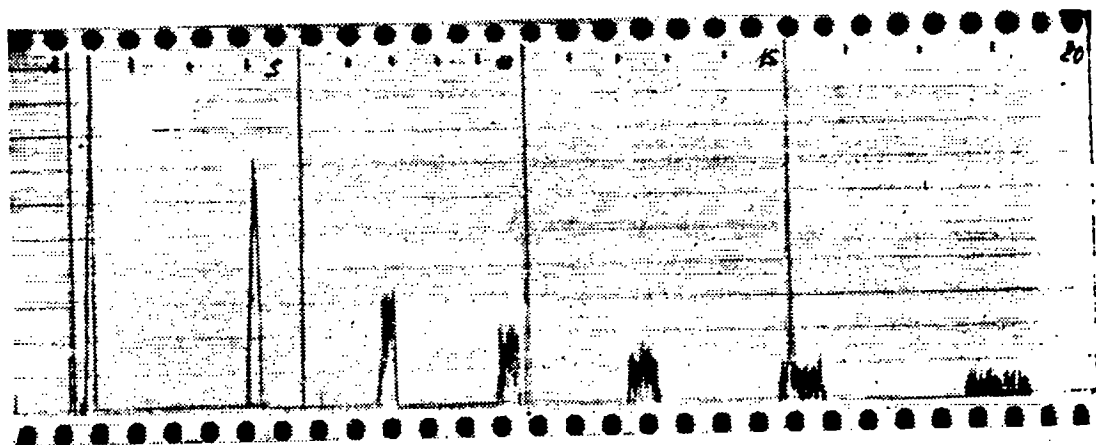


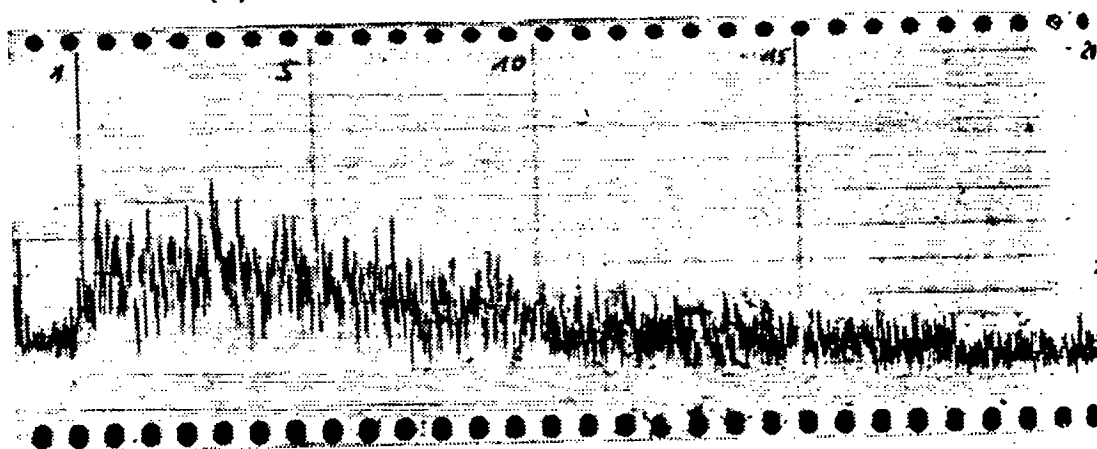
Figure 15. - Autocorrelation functions of a sequence of impulses.



(a) Release of impulses through sine voltage.

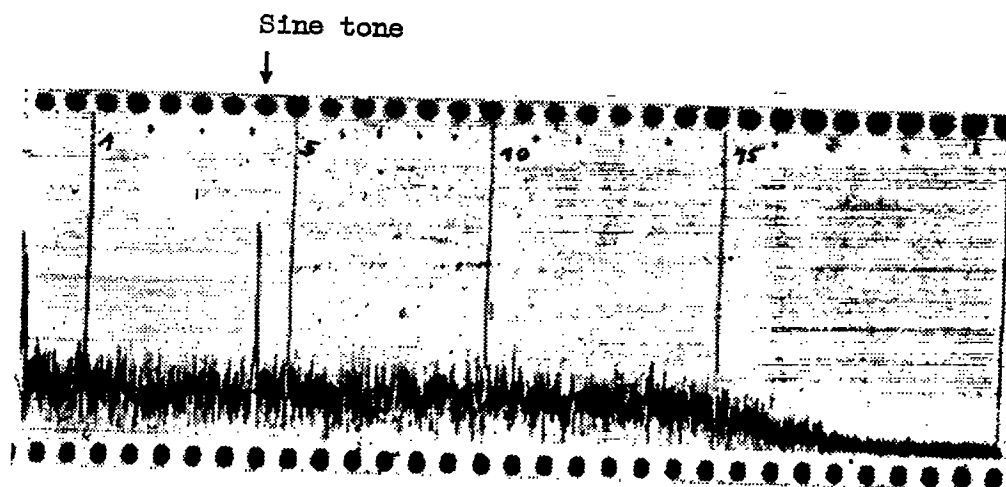


(b) Release of impulses through wobble tone.

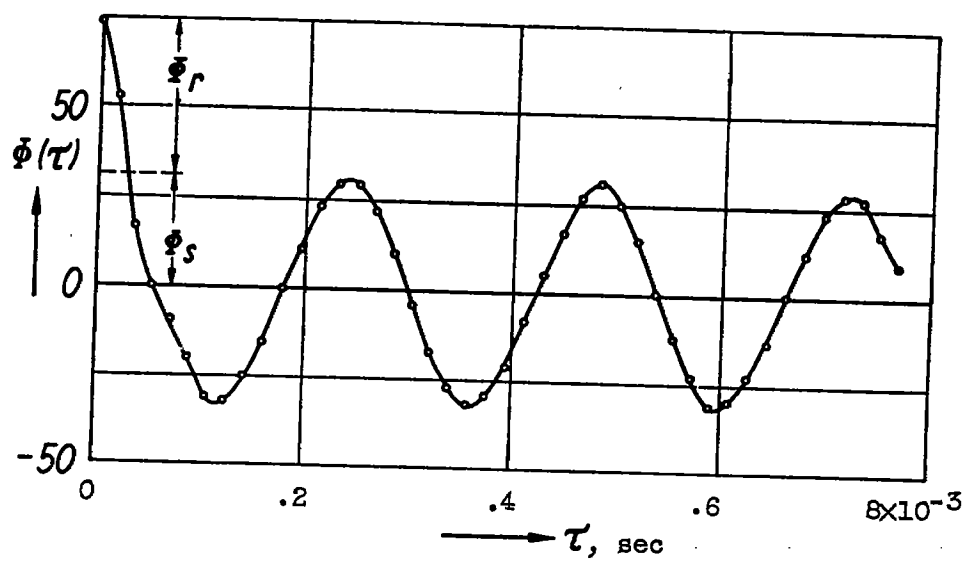


(c) Release of impulses through noise voltage.

Figure 16. - Sound analysis of sequences of impulses.

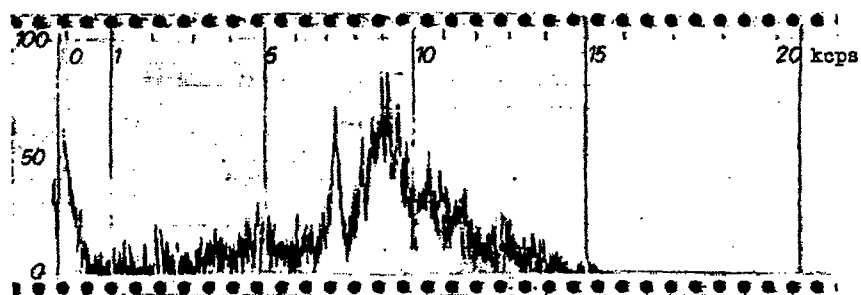


(a) Spectrum.

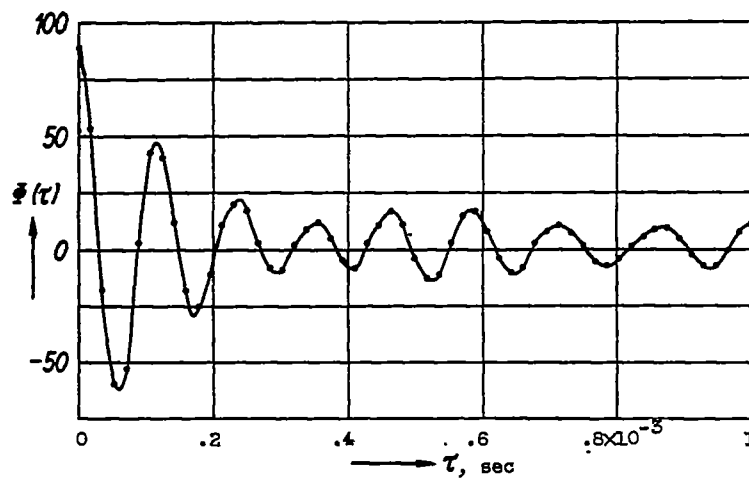


(b) Autocorrelation analysis.

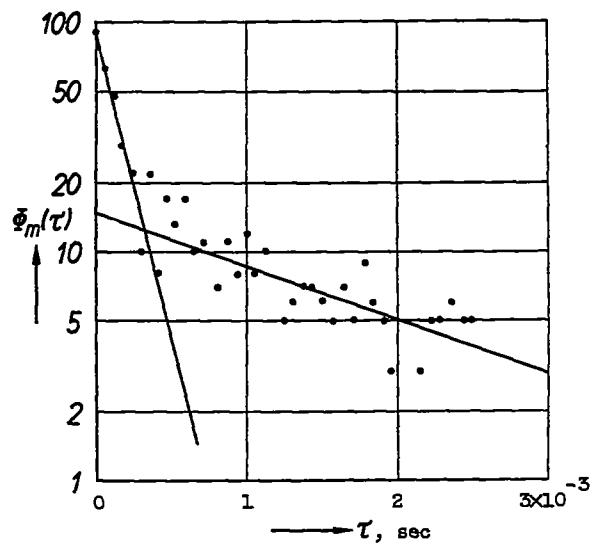
Figure 17. - Sine tone with superposed noise.



(a) Spectrum.



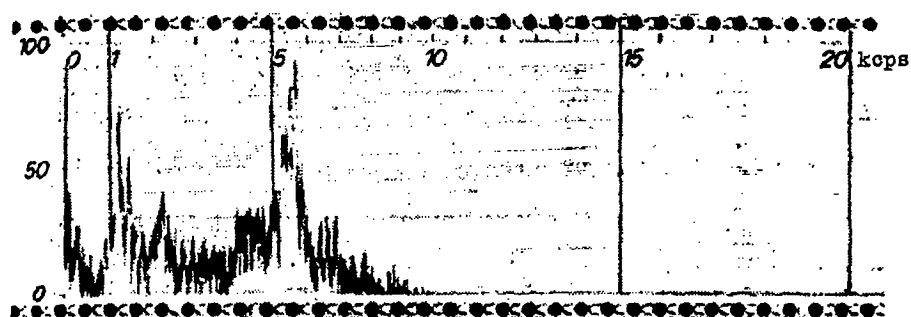
(b) Autocorrelation function (linear scale).



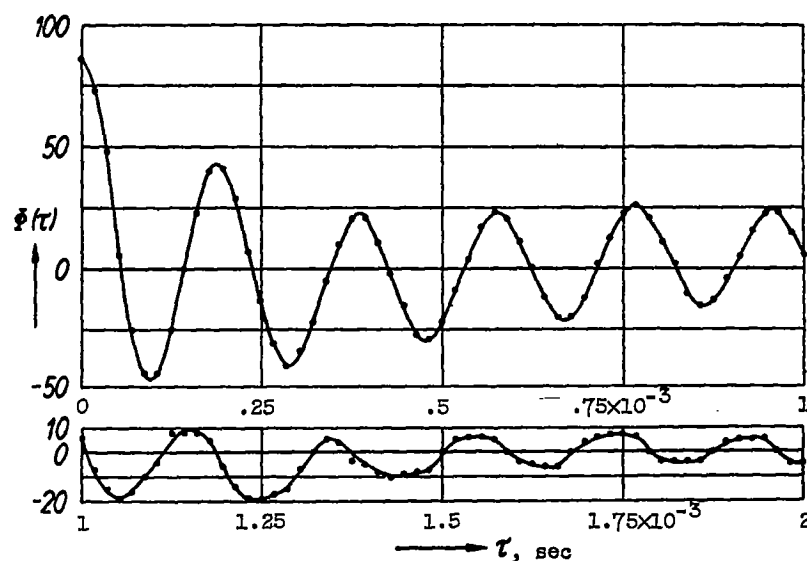
(c) Extreme values of autocorrelation function in logarithmic scale.

Figure 18. - Analysis of a time function consisting of two narrow frequency bands (voiceless "s").

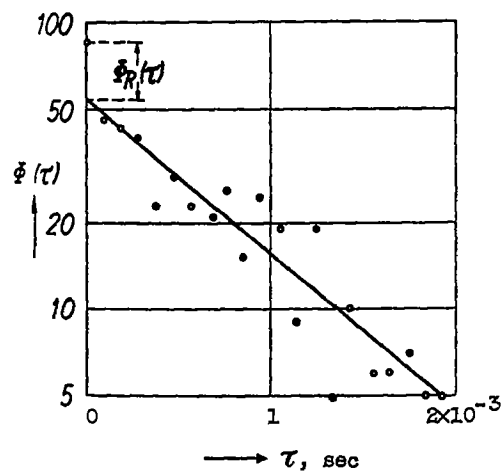




(a) Spectrum.

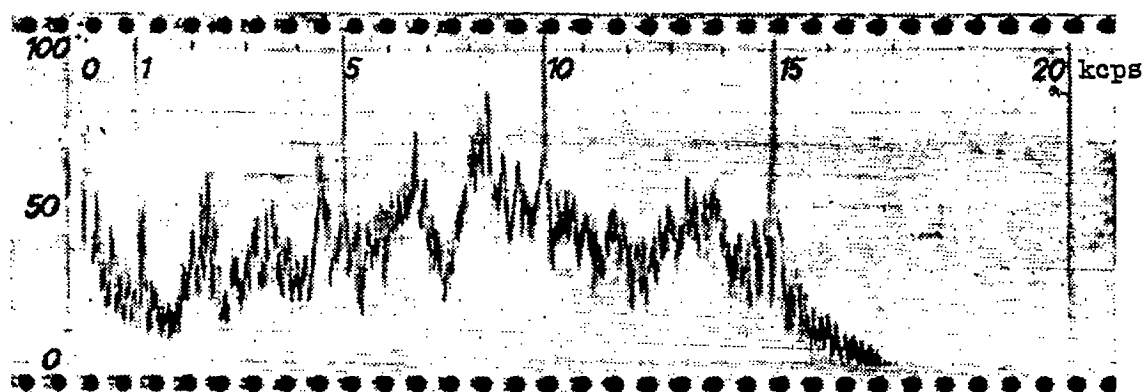


(b) Autocorrelation function (linear scale).

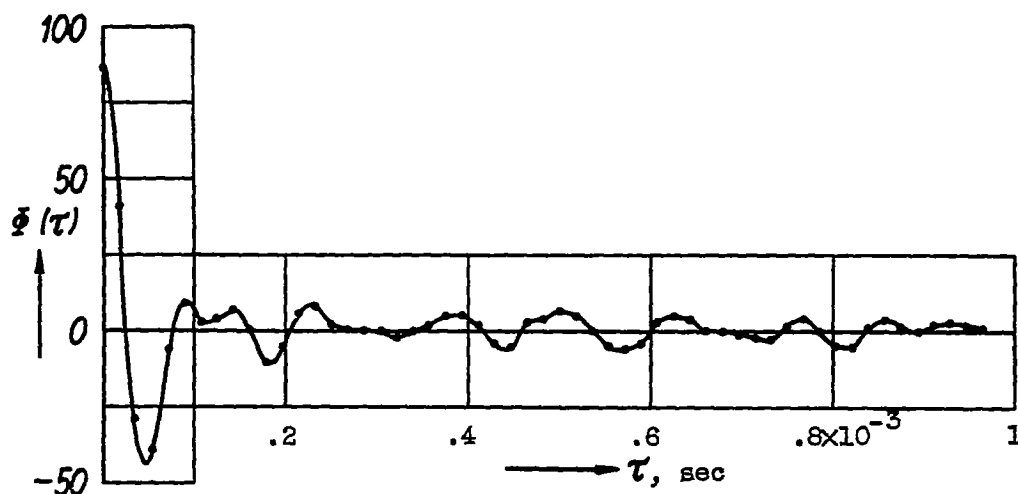


(c) Extreme values of autocorrelation function in logarithmic scale.

Figure 19. - Voiceless "sh."

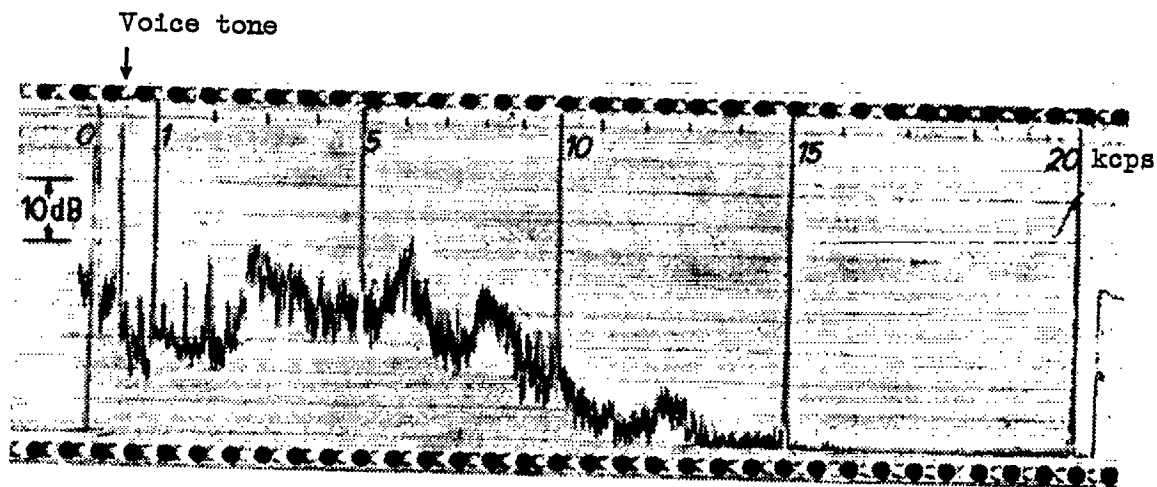


(a) Spectrum

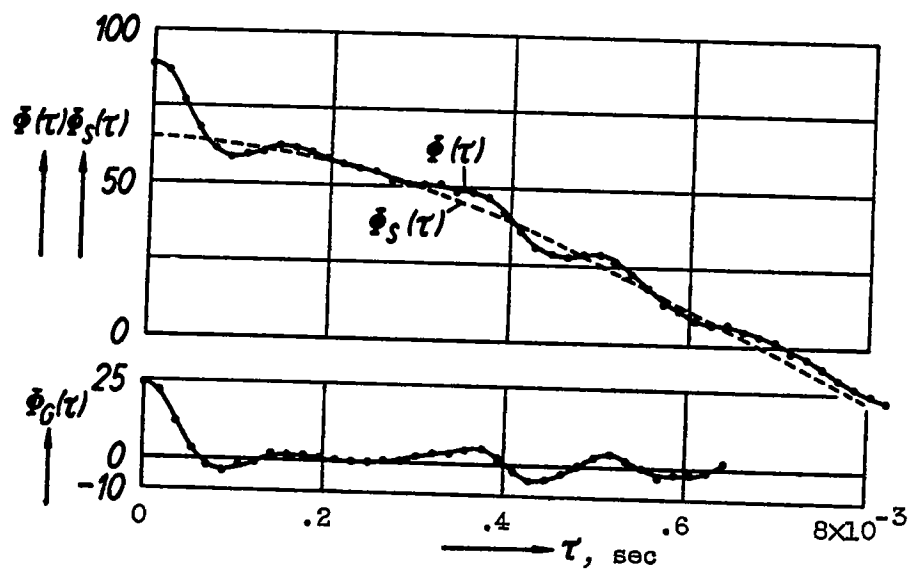


(b) Autocorrelation function.

Figure 20. - Voiceless "f."

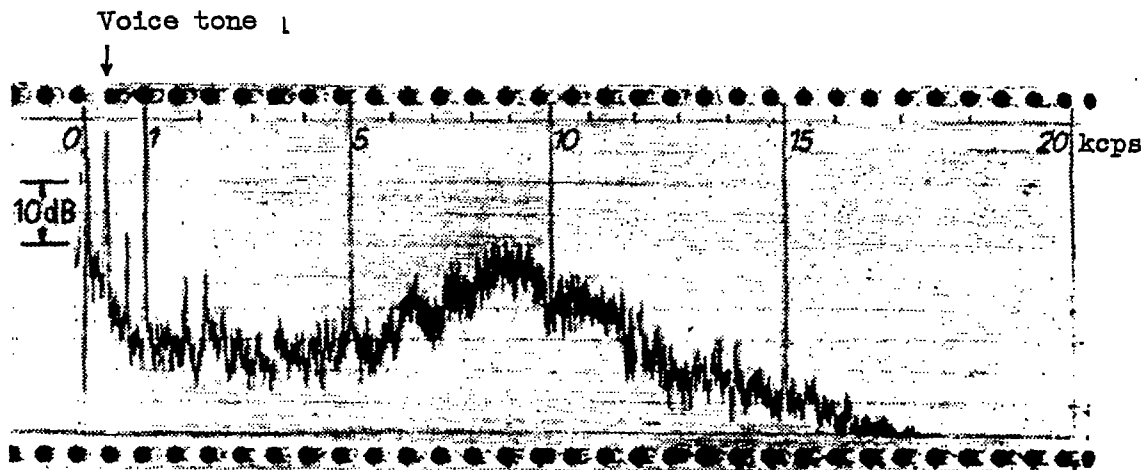


(a) Spectrum (logarithmic scale).

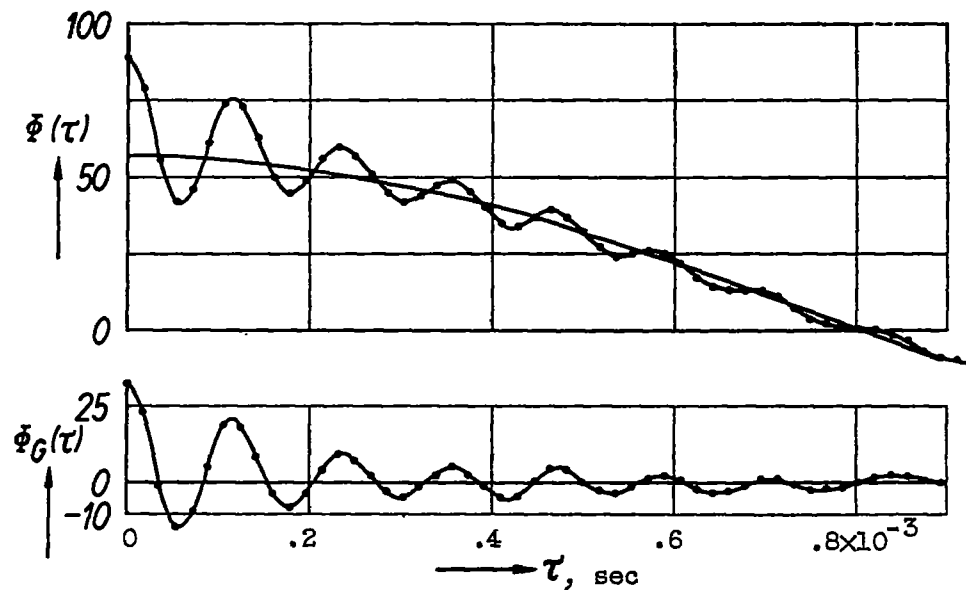


(b) Above: measured autocorrelation curve.  
Below: autocorrelation function  $\phi_G$  of noise component (component of voice tone removed).

Figure 21. - Voiced "sh" ("j" in French "jour.").

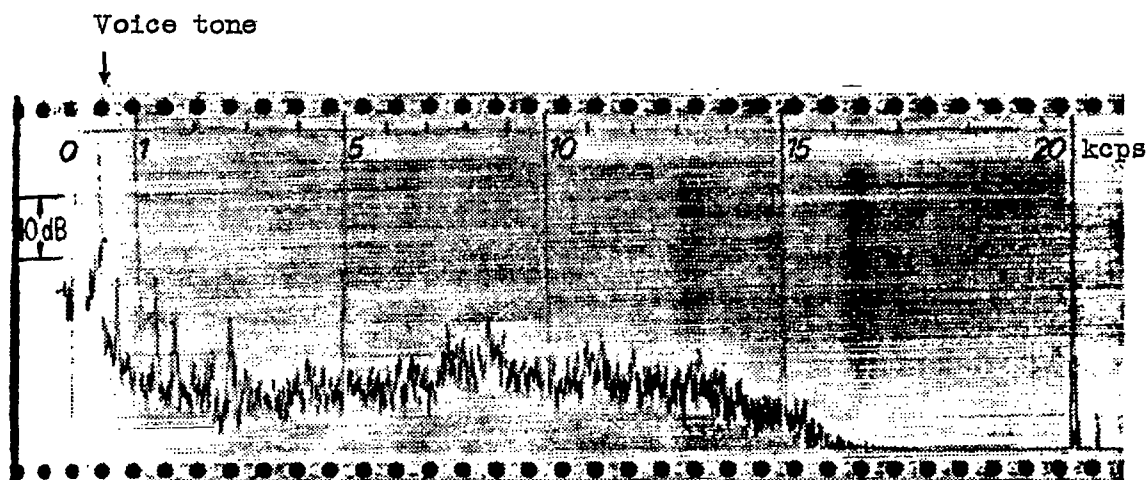


(a) Spectrum (logarithmic scale).

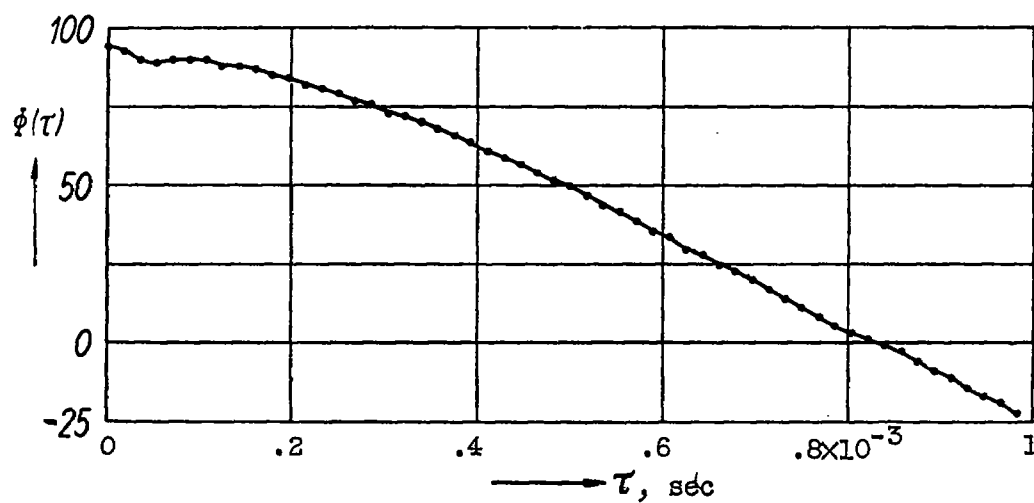


(b) Above: measured autocorrelation curve.  
 Below: autocorrelation curve of noise component.

Figure 22. - Voiced "s" ("z").



(a) Spectrum (logarithmic scale).



(b) Autocorrelation function.

Figure 23. - Voiced "r" ("v").